# การผลิตแก๊สไฮโดรเจนพร้อมกับสังกะสีออกไซด์ขนาดนาโนโดยการไฮโดรไลซิสของไอสังกะสี

นางสาวศิริวิมลธนาจิรวัฒน์

วิทยานิพนธ์นี้เป็นส่วนหนึ่งของการศึกษาตามหลักสูตรปริญญาวิศวกรรมศาสตรมหาบัณฑิต
สาขาวิชาวิศวกรรมเคมี ภาควิชาวิศวกรรมเคมี
คณะวิศวกรรมศาสตร์ จุฬาลงกรณ์มหาวิทยาลัย
ปีการศึกษา 2554

# SIMULTANEOUS PRODUCTION OF HYDROGEN AND NANOSIZED ZINC OXIDE BY HYDROLYSIS OF ZINC VAPOR

Miss Siriwimol Thananjirawat

A Thesis Submitted in Partial Fulfillment of the Requirements
for the Degree of Master of Engineering Program in Chemical Engineering
Department of Chemical Engineering
Faculty of Engineering
Chulalongkorn University
Academic Year 2011

| | |
|---|---|
| Thesis Title | SIMULTANEOUS PRODUCTION OF HYDROGEN AND NANOSIZED ZINC OXIDE BY HYDROLYSIS OF ZINC VAPOR |
| By | Miss Siriwimol Thanajirawat |
| Field of Study | Chemical Engineering |
| Thesis Advisor | Assistant Professor Varong Pavarajarn, Ph.D. |
| Thesis Co-advisor | Professor Suttichai Assabumrungrat, Ph.D. |

---

Accepted by the Faculty of Engineering, Chulalongkorn University in Partial Fulfillment of the Requirements for the Master's Degree

…….....Dean of the Faculty of Engineering
(Associate Professor Boonsom Lerdhirunwong, Dr.Ing.)

THESIS COMMITTEE

…….. Chairman
(Apinan Soottitantawat, D.Eng.)

…….……. Thesis Advisor
(Assistant Professor Varong Pavarajarn, Ph.D.)

…….. Thesis Co-advisor
(Professor Suttichai Assabumrungrat, Ph.D.)

…….. Examiner
(Associate Professor Tawatchai Charinpanitkul, D.Eng.)

…….. External Examiner
(Associate Professor Navadol Laosiripojana, Ph.D.)

ศิริวิมล ธนาจิรวัฒน์ : การผลิตแก๊สไฮโดรเจนพร้อมกับสังกะสีออกไซด์ขนาดนาโนโดยการไฮโดรไลซิสของไอสังกะสี. (SIMULTANEOUS PRODUCTION OF HYDROGEN AND NANOSIZED ZINC OXIDE BY HYDROLYSIS OF ZINC VAPOR)
อ. ที่ปรึกษาวิทยานิพนธ์หลัก : ผศ.ดร.วรงค์ ปวราจารย์, อ. ที่ปรึกษาวิทยานิพนธ์ร่วม : ศ.ดร.สุทธิชัย อัสสะบำรุงรัตน์, 86 หน้า.

แก๊สไฮโดรเจนสามารถผลิตขึ้นพร้อมกับสังกะสีออกไซด์ขนาดนาโนโดยการไฮโดรไลซิสของไอสังกะสี กับไอน้ำ โดยการทดลองนี้ใช้เครื่องปฏิกรณ์แบบท่อ สังกะสีถูกทำให้เป็นไอที่อุณหภูมิต่ำกว่าจุดเดือด และ ป้อนเข้าสู่บริเวณที่จะเกิดปฏิกิริยาโดยแก๊สเฉื่อย ส่วนไอน้ำที่ถูกสร้างขึ้นจะถูกแยกส่งเข้าไปบริเวณที่จะเกิดปฏิกิริยา ในทิศทางเดียวกันกับการไหลของไอสังกะสี ผลิตภัณฑ์ของแข็งที่เก็บได้จากชุดกรองจะถูกนำไปวิเคราะห์โดยใช้เครื่อง วิเคราะห์การกระเจิงของรังสีเอกซ์ และ กล้องจุลทรรศ อิเล็คตรอนแบบส่องกราด ในขณะที่ผลิตภัณฑ์ที่เป็นแก๊สจะถูกวิเคราะห์โดยใช้เครื่อง แก๊สโคร มาโทกราฟ ซึ่งในการทดลองนี้ ได้ศึกษาผลของ อุณหภูมิในการระเหยสังกะสี อุณหภูมิในการทำปฏิกิริยา ความเร็วของไอสังกะสี และ เวลาในการเกิดปฏิกิริยา ซึ่งจากการทดลองพบว่า เมื่อลดอุณหภูมิในการระเหยสังกะสี ทำให้แก๊สไฮโดรเจนที่ผลิตได้น้อยลง เมื่อเพิ่มอุณหภูมิในการเกิดปฏิกิริยาจาก 500 เป็น 900 องศาเซลเซียส จะส่งผลทำให้ ผลได้ของแก๊สไฮโดรเจนที่ผลิตได้เพิ่มขึ้นจาก 24.4 เป็น 59.71 เปอร์เซนต์ ในขณะที่สัดส่วนของสังกะสีออกไซด์ที่ดักเก็บได้เพิ่มขึ้นจาก 16.9 เป็น 30.71 เปอร์เซนต์ และเมื่อเพิ่มความเร็วของไอสังกะสี จะทำให้แก๊สไฮโดรเจนที่ผลิตได้มีค่าลดลง ซึ่งผลได้แก๊สไฮโดรเจนที่ผลิตได้สูงสุดมีค่า 72.59 เปอร์เซนต์ ของค่าทางทฤษฎี

ภาควิชา..... ลายมือชื่อนิสิต.....
สาขาวิชา...วิศวกรรมเคมี..... ลายมือชื่อ อ.ที่ปรึกษาวิทยานิพนธ์หลัก.....
ปีการศึกษา..2554..... ลายมือชื่อ อ.ที่ปรึกษาวิทยานิพนธ์ร่วม.....

# # 5270524621 : MAJOR CHEMICAL ENGINEERING
KEYWORDS : ZINC OXIDE/ HYDROGEN PEODUCTION/ HYDROLYSIS/ NANOPARTICLE

SIRIWIMOL THANAJIRAWAT : SIMULTANEOUS PRODUCTION OF HYDROGEN AND NANOSIZED ZINC OXIDE BY HYDROLYSIS OF ZINC VAPOR. ADVISOR : ASST. PROF.VARONG PAVARAJARN, Ph.D., CO ADVISOR : PROF.SUTTICHAI ASSABUMRUNGRAT, Ph.D., 86 pp.

Hydrogen and zinc oxide (ZnO) nanoparticles were simultaneously produced by the steam-hydrolysis of zinc vapor. This process was experimentally demonstrated using a tubular flow reactor. Zinc vapor was evaporated at temperature below its boiling point and carried to the reaction zone by an inert carrier gas. Steam was generated in separated vessel and fed co-currently with the zinc vapor into the reaction zone. Solid products collected by filter downstream were characterized by X-ray diffraction and scanning electron microscopy (SEM) while the gas was periodically sampled and analyzed by gas chromatography (GC). In this research influence of process parameters including zinc evaporation temperature, reaction temperature, flow rate of zinc vapor, and resident time were investigated. The experimental results show that low zinc evaporation temperature resulted in decreased yield of $H_2$. By increasing the reaction temperature from 500$^o$C to 900$^o$C, the yield of $H_2$ increased from 24.4% to 59.71%, while the fraction of ZnO within the collected products increased from 16.9% to 30.71 %. Higher carrier gas flow rate resulted in lower achieved yield of $H_2$ and smaller particle size. The highest yield of $H_2$ production achieved was 72.59% with respect to theoretical value.

Department : Chemical Engineering Student's Signature .....
Field of Study : Chemical Engineering Advisor's Signature .....
Academic Year : 2011 Co-advisor's Signature .....

## ACKNOWLEDGEMENTS

The author is very thankful to my thesis advisor and co-advisor, Asst Prof. Varong Pavarajarn, and Prof. Suttichai Assabumrungrat Department of Chemical Engineering, Chulalongkorn University, for their introducing me to this interesting project, and for their helpful and stimulated suggestions, deep discussion and encouraging guidance throughout the course of this work. Furthermore, the author is also thankful to Dr. Apinan Soottitantawat as the chairman, Assoc Prof. Tawatchai Charinpanitkul and Assoc Prof. Navadol Laosiripojana for their simulative comments and participation as my thesis committee.

Furthermore, the author would like to acknowledge financial support from the centenary fund of Chulalongkorn University and Univenture Public Co., Ltd. to support zinc foil as raw material.

Most of all, the author wishes to thank the members of the Center of Excellence in Particle Technology and members of Excellence on Catalysis and Catalytic Reaction Engineering, Department of Chemical Engineering, Faculty of Engineering, Chulalongkorn University for their assistance.

Finally, the author would like to express her highest gratitude to her parents who always pay attention to her all the times for suggestions and their wills. The most success of graduation is devoted to her parents.

# CONTENTS

Page

**CHAPTER** Page

# LIST OF TABLES

Page

## LIST OF FIGURES

Page

Page

Page

Page

# CHAPTER I

## INTRODUCTION

Zinc oxide is an inorganic compound with the formula ZnO. It usually appears as a white powder, nearly insoluble in water. As a highly applicable and widely used II–VI semiconducting material, ZnO, with a wide band gap (3.37 eV) and high exciton binding energy (60 meV) is an excellent candidate for the fabrication of nanoelectronic and photonic devices. Because of its wide band gap and high exciton binding energy that is much larger than ZnSe (22 meV) and GaN (25 meV), it has been recognized as a versatile material. ZnO is also acknowledged for its catalytic, electrical, optoelectronic, sensing and photochemical properties. For ZnO, different nanostructures, such as nanorods, nanoneedles, whiskers structures, ribbon/comb structures, tetrapods, etc., can be obtained under different synthesis routes and conditions. Noted that ZnO is the third largest aerosol-made commodity by volume [1] produced by the so-called French and American processes, leading to micron-sized particles that are used mostly as vulcanizing agents for tires. ZnO nanoparticles, as used in electronics, optics, and photonics, are produced by wet-phase processes [2], thermal evaporation [3] , Metal Organic Chemical Vapor Deposit (MOCVD) [4], hydrothermal synthesis [5] and hydrolysis of zinc vapor [6].

Hydrolysis of zinc vapor to zinc oxide is an exothermic reaction that releases $H_2$, which is quite attractive for its potential in achieving high energy conversion efficiencies [7]. Hydrogen formation by Zn vapor hydrolysis, however, has been reported in hot-wall aerosol reactors resulting in ZnO deposition on the reactor walls, making ZnO recovery and recycling rather difficult [8]. Very recently, $H_2$ has been produced continuously in hot-wall aerosol flow reactors by evaporating and subsequent in-situ hydrolyzing of Zn with a conversion rate of 70% with respect to zinc as the limiting reactant [8].

The present research explores the simultaneous production of hydrogen and nanosized zinc oxide by hydrolysis of zinc vapor. Effects of flow rate of carried gas (Ar), evaporation temperature for zinc, reaction temperature and reaction time will be investigated.

**Objectives of research**

Objective of this research is to investigate the hydrolysis of zinc vapor by steam to simultaneously produce ZnO nanoparticles and $H_2$ gas products.

**Scopes of research**

ZnO nanoparticles and $H_2$ are synthesized from the reaction between zinc vapor, evaporated from 99.99% zinc foil, and steam supplied to the reactor. The following synthesis parameters are investigated for synthesized ZnO nanoparticle and $H_2$,

1. Hydrolysis of Zn vapor in steady-flow condition

    - Zn evaporation temperature : 600 – 850 $^{o}$C
    - Reaction temperature : 500 - 1200 $^{o}$C
    - Flow rate of carrier gas for zinc vapor : 0.5, 1, 1.5 l/min
    - Residence time : 1 – 3 s

2. The ZnO nanoparticles will be characterized by the following techniques

    - X-ray diffraction (XRD) for determining lattice parameters.
    - Scanning electron microscopy (SEM) for observing the size and shape of ZnO particles.

- Inductive Coupled Plasma Optical Emission Spectrometer (ICP-OES) for determining the actual amount of ZnO particles.

3. The $H_2$ production will be characterized by Gas Chromatography (GC)

**Benefits of research**

Zno will be synthesized by the hydrolysis Zn vapor with steam and $H_2$ gas will be by- product of reaction. The understanding of the effect of various operating parameters can lead to the control of the chemical and physical properties of products simply by adjusting process parameters.

# CHAPTER II

## FUNDAMENTAL KNOWLEDGE AND LITERATURE REVIEW

### 2.1 Zinc Oxide (ZnO)

Zinc oxide is a unique modern material. It has such an array of properties that continue to increase in usefulness of ZnO in many of the ever-widening fields of science and technology. It is a chemical compound with formula ZnO. It is nearly insoluble in water but soluble in acid or alkalis. It is a fluffy, white powder commonly known as zinc white as shown in Figure 2.1. Crystalline ZnO exhibits the piezoelectric effect and its color will change from white to yellow when heated, and come back to white when cooled down. ZnO will decompose into zinc vapor and oxygen at around 1975 °C.


**Figure 2.1** Zinc oxide powder

## 2.2 Crystal Structure and Lattice Parameters of Zinc Oxide

At ambient pressure and temperature, ZnO crystallizes in the wurtzite structure, as shown in Figure 2.2. This is a hexagonal lattice characterized by two interconnecting sublattices of $Zn^{2+}$ and $O^{2-}$ such that each Zn ion is surrounded by a tetrahedral of O ions. In addition to the wurtzite phase, ZnO is also known to crystallize in the cubic zinc blende and rocksalt structures, which are illustrated in Figure 2.3 and 2.4 respectively. Zinc blende ZnO is stable only by growth on cubic structures, while the rocksalt structure is a high-pressure metastable phase forming at pressure about 10 GPa, and cannot be epitaxially stabilized. Theoretical calculations have indicated that the wurtzite form is energetically preferable compared to zinc blende and rocksalt.

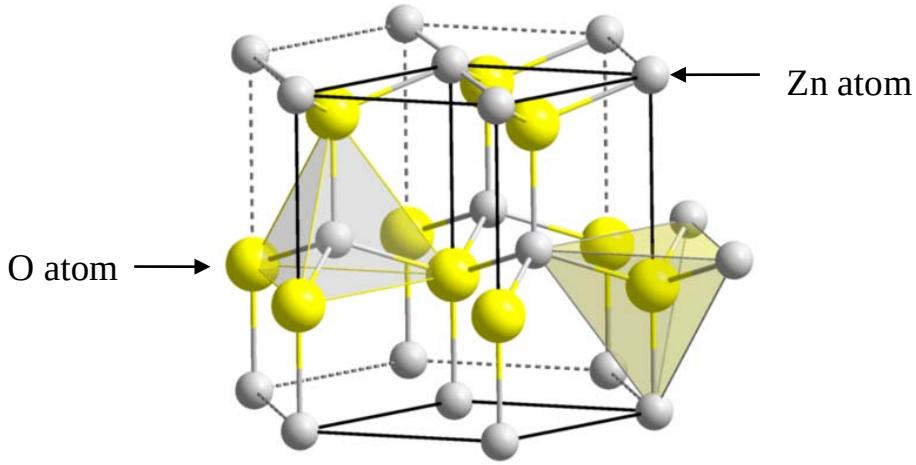


**Figure 2.2** The hexagonal wurtzite structure of ZnO.

**Ref:** http://wapedia.mobi/en/File:Wurtzite_polyhedra.png

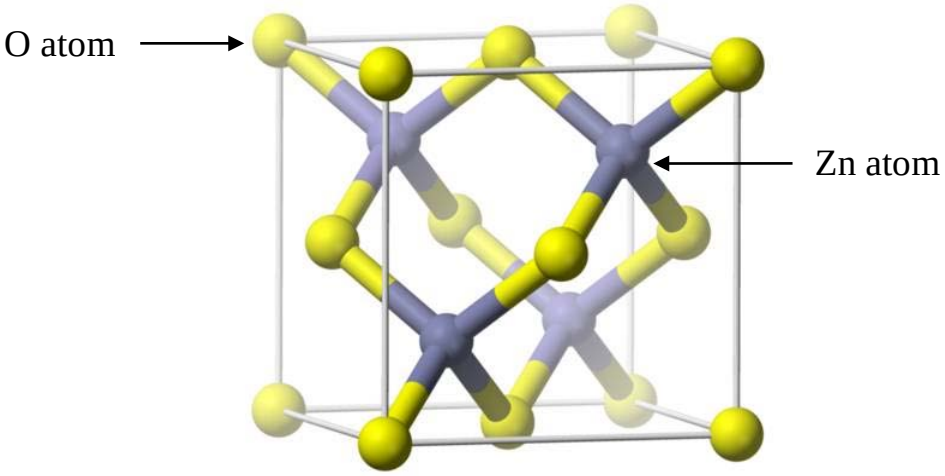


**Figure 2.3** zinc blende phase of ZnO.

**Ref:** http://wapedia.mobi/en/File:Zinc blende polyhedra.png

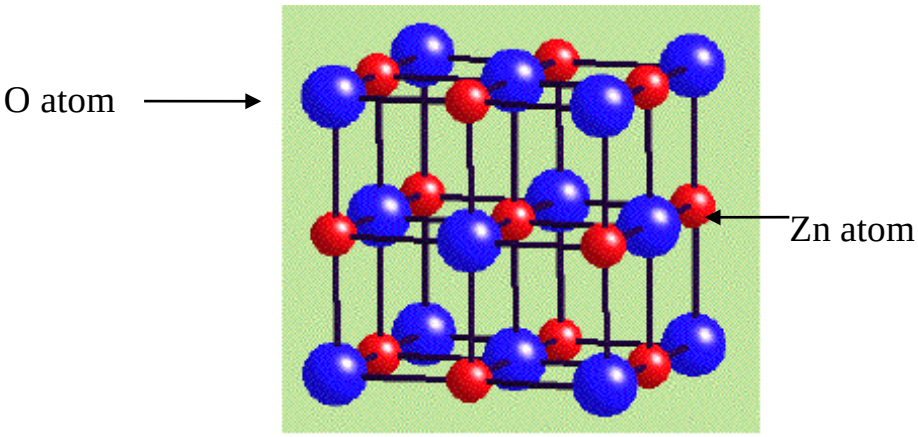


**Figure 2.3** The rock salt phase of ZnO.

**Ref:** www.chem.ox.ac.uk

## 2.3 Properties of Zinc Oxide

Zinc oxide is an n-type semiconductor with a band gap of 3.37 eV and the free exciton energy of 60 meV, which makes it very high potential for room temperature light emission. This also gives zinc oxide strong resistance to high temperature electronic degradation during operation. Therefore, it is attractive for many optoelectronic applications in the range of blue and violet light as well as UV devices for wide range of technological applications**.** Zinc oxide also exhibits dual semiconducting and piezoelectric properties. The other properties are given in Table 2.1

**Table 2.1** Properties of wurtzite zinc oxide

| *Property* | *Value* |
|---|---|
| Lattice parameters at 300 K | |
| *a* | 0.32495 nm |
| *c* | 0.52069 nm |
| *a/c* | 1.602 (ideal hexagonal structure is 1.633) |
| Density | 5.606 g/cm$^3$ |
| Melting point | 1975 $^o$C |
| Thermal conductivity | 130 W/m.K |
| Linear expansion coefficient (/$^o$C) | *a*: 6.5 x 10$^{-6}$ |
| | *c*: 3.0 x 10$^{-6}$ |
| Static dielectric constant | 8.656 |
| Energy gap | 3.37 eV, direct |
| Exciton binding energy | 60 meV |

Zinc oxide occurs in nature as mineral. Zinc oxide is prepared in industrial scale by vaporizing zinc metal and oxidizing the generated zinc vapor with preheated air. Zinc oxide has numerous industrial applications. It is a common white pigment in paints. It is used to make enamel, white printing ink, white glue, opaque glasses, and floor tiles. It is also used in batteries, electrical equipments, piezoelectric devices, cosmetics, dental cements, and pharmaceutical applications such as antiseptic and astringent. Other applications are the use as flame retardant, and UV absorber in plastics. Nevertheless, the current major application of zinc oxide is in the preparation of most zinc salts.

## 2.4 Commercial Process of synthesize ZnO

### *2.4.1 French Process*

In French process, zinc metal is vaporized in suitable containers by external heating, after which the vapor is burned in air in an adjoining off-take pipe or combustion chamber to form fine zinc oxide powder. Temperature and speed of mixing of air and vapor are important factors to control particle size. The higher temperature brings about the finer particle size of the resulting ZnO product. For the commercial practice, the system (Figure 2.5) is consisted of a graphite crucible placed inside a cylindrical firebrick furnace. The design is a muffle type whereby hot flame from a burner heats up the crucible by convection, and heat is transferred to the zinc ingots (inside the crucible) via conduction through the graphite lining. Zinc melts at 420$^{o}$C with heat of fusion of 6.67 kJ/mol, boils at 907$^{o}$C with heat of vaporization of 114.2 kJ/mol, and its critical temperature is 3107$^{o}$C. The crucible is covered with a graphite lid in order to pressurize the zinc vapor trapped inside the crucible. Once the lid orifice is removed, the pressure difference causes the zinc vapor to purge out and it is instantaneously oxidized by ambient air. The zinc vapor has a nozzle temperature of 1100-1400$^{o}$C and a nozzle speed of about 8-12 m/s (calculated). An enclosure is sometimes built around the combustion chamber in order to control the oxygen-to-zinc ratio and to stabilize the temperature.

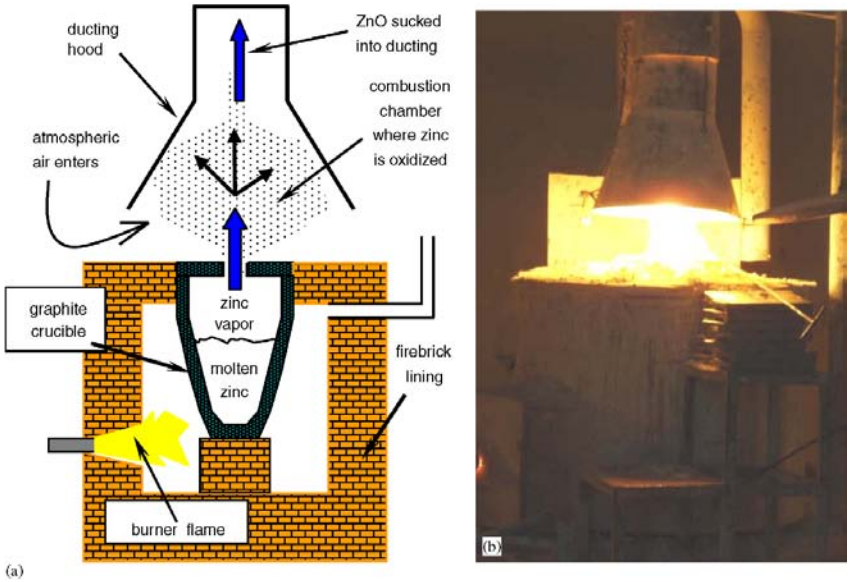


(a) (b)

**Figure 2.5** (a) Schematic of French process furnace and (b) furnace in operation. [10]

Oxidation of zinc oxide and the growth of zinc oxide crystals take place in the combustion area. The temperature drags from 1100$^{o}$C to 800$^{o}$C between the crucible orifice and the top part of the conical suction hood (Figure 2.5(a)) within seconds. Despite the highly nonuniform crystallization nature of this rapid *subminute* growth process, a large variety of nanostructure of ZnO, which includes nanorods, nanoplates, nanoboxes, irregularly shaped particles (ISPs), polyhedral drums and nanomallets can be formed. Mahmud et al. synthesized ZnO by the French process. The morphologies of ZnO were rod, polyhedral drum, irregularly-shaped particles, nanoplate, nanobox, and nanomallet [9].

The powder is collected by filtration through a multiplicity of textile bags. Frequent shaking of the bags prevents excessive cake build-up and drops the oxide into collection receptacles. In some plants, the baghouse is preceded by a series of settling chamber or baffled tunnels, in which the bulk of the production is collected. In either case, the oxide can be collected on a grade basis. The fluffiest product is gathered at the farthest distance from the combustion area. Preparation of zinc oxide

from metal permits considerable flexibility in control of particle size, particle shape, and product purity. For example, average particle size may range from 0.1 micron to several microns. The larger sizes are produced by maintaining the oxide at elevated temperature for longer period of time.

### *2.4.2 American Process*

For American process, oxidized ores or roasted sulfide concentrates are mixed with coal (anthracite) and smelted in a Wethreill-type flat-bed or other type of furnace. The coal and the products of partial combustion, particularly carbon monoxide, reduce the ore to zinc vapor. In the off-take pipe, the vapor together with the gases from the coal, are burned under controlled conditions and piped to the baghouse, where the zinc oxide is collected. The american process oxide is characterized by the presence of sulfur compounds in zinc, such as zinc-based sulfates preferred by some producers of rubber and paint products.

## 2.5 Generation of Particles by Reaction in Gas Phase

Particles synthesis from vapor phase involves the processes of seed generation and particle growth. The processes involving in particles synthesis from the vapor phase are summarized in Figure 2.6**.** Seed particles are frequently produced by a burst of homogeneous nucleation of vapor phase species. Growth can involve the processes of physical vapor deposition (PVD) or chemical vapor deposition (CVD) of vapor phase species or coagulation, which is the collisional aggregation of small particles to form larger ones. The latter process dominates when large numbers of particles are formed in the nucleation burst. Coagulation of the solid particles often results in the formation of agglomerates particles comprised of the large number of smaller primary particles. Such agglomerates formation frequently begins after a period of coalescent coagulation in high-temperature regions of the reactor, leading to a relatively uniform primary particle size which is sometime misinterpreted as evidence that coalescent has ceased. Instead, coagulation accelerates once agglomerates begin to form due to

the increased projected areas that result from agglomerate formation. Strong bonds can form between the primary particles by solid phase sintering, leading to hard agglomerates that are often difficult to disperse.

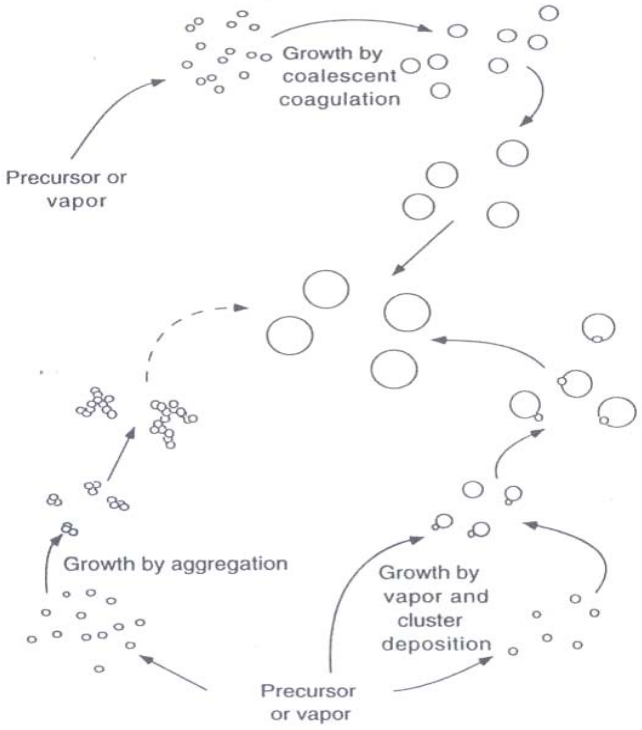


**Figure 2.5** Mechanisms of particle formation and growth from vapor-phase precursors.

### 2.6 Synthesis of ZnO Nanostructures

Various methods have been used for the production of ZnO nanostructures. They can be grouped in two main categories: high-temperature techniques, such as chemical vapor deposition, pulsed-laser deposition and thermal evaporation where the growth temperature is higher than 400$^{o}$C, and chemical solution methods at around 100$^{o}$C. The first category utilizes expensive equipment and is energy consuming, while the latter often requires liquid-phase coating of the substrates with ZnO seeds, which is a quite complex procedure.

### *2.6.1 Thermal oxidation process*

The most common method to synthesize ZnO nanostructures. Zn and oxygen are transported and react with each other, forming ZnO nanostructures. There are several ways to generate Zn and oxygen vapor. Decomposition of ZnO is a direct and simple method, however, it is limited to very high temperature (~1400$^{o}$C). Another direct method is to heat up Zn powder under oxygen flow. This method facilitates relative low growth temperature (500-700$^{o}$C), but the ratio between the Zn vapor pressure and oxygen pressure needs to be carefully controlled in order to obtain desired ZnO nanostructures. It has been observed that the change of this ratio contributes to a large variation on the morphology of nanostructures. The indirect methods to provide Zn vapor include metal-organic vapor phase epitaxy, in which organometallic Zn compound, diethylzinc for example, is used under appropriate oxygen of $N_2O$ flow. Also in the widely used carbothermal method, ZnO powder is mixed with graphite powder as source material. At about 800-1100$^{o}$C, graphite reduces ZnO to form Zn and $CO/CO_2$ vapors, which later react together and result in ZnO nanocrystals. The advantages of this method lie in that the existence of graphite significantly lowers the decomposition temperature of ZnO.

### *2.6.2 Hydrolysis of zinc vapor*

Hydrolysis of zinc vapor to zinc oxide is an exothermic reaction that releases $H_2$, which is quite attractive for its potential in achieving high energy conversion efficiencies [7]. Hydrogen formation by Zn vapor hydrolysis, however, has been reported in hot-wall aerosol reactors resulting in ZnO deposition on the reactor walls, making ZnO recovery and recycling rather difficult [8].

2.6.2.1 Effect of Reaction Temperature

Wegner et al. presented a novel reactor concept for the production of high-purity hydrogen by hydrolysis of Zn [11]. It features three temperature-controlled zones that could overlap,i.e., a Zn nanoparticle-$H_2O$ (g) mixing zone, a Zn-nanoparticle formation by steam-quenching zone, and a Zn (g)–$H_2O$ reaction zone. This combined process offered Zn nanoparticles with high specific surface area for enhanced interface reaction kinetics and, consequently, high degree of chemical conversion. Additional advantages are pertinent to the process technology aspects of having a simple, controllable, and continuous feeding of reactants and removal of products.

Two reaction mechanisms were proposed: (1) reaction between Zn (g) and steam ($T_{reac}$ 923 $^oC$) by chemical vapor deposition at the surface of the reactor walls at temperature above saturation point of Zn vapor, and (2) reaction between Zn (l) or Zn (s) particles and steam ($T_{reac}$ below 923 $^oC$) at the particle surface at temperatures below saturation point of Zn vapor. The results indicated particles formation by homogeneous nucleation followed by condensation and/or coagulation and deposition at the reactor walls. The first reaction mechanism yielded 100% Zn-conversion, but might not be practically applicable in large-scale industrial processes due to the formation of hard ZnO deposits. The latter, industrially preferred mechanism for continuous mode operation, yielded up to 83% Zn-conversion. Zn conversion decreased with decreasing reactor temperature and increasing residence time as a result of the formation of a ZnO passivating layer on larger Zn particles. This undesired reaction barrier could in principle be minimized by reducing the size of formed nanoparticles and controlling the reactor temperature. The average $H_2$ yield after a single pass of $H_2O$ of 0.85 s residence time reached 60% (peaked 70%) [11].

Steinfeld et al. proposed simultaneous synthesis of $H_2$ and ZnO nanoparticles that was investigated by steam-hydrolysis of Zn vapor in a hot-wall aerosol flow reactor with separated evaporation, cooling, and reaction zones. Superheated Zn vapor was carried by Ar into a tubular, quartz reactor where it was mixed and quenched by a superheated, equimolar $H_2O$/Ar stream, resulting in Zn/ZnO nanoparticles and $H_2$.

The Zn (g) vapor was generated by electric heating of a Zn crucible whose weight was continuously monitored and compared to $H_2$ production rate. The reactor was operated at 1 bar and 573–1273 K: temperature above and below saturation point of Zn vapor, Zn aerosol formation by condensation taking place in parallel with the omnipresent ZnO formation by gas phase or surface hydrolysis of Zn. The variable cooling zone length (LC) was used to select process conditions with and without Zn particle formation before hydrolysis. It was found that increasing the reaction zone temperature favored $H_2$ formation (yielded up to 90% $H_2$ conversion) and enhanced the ZnO fraction in the product particles at the expense of particle yield. Because $H_2$ formation by Zn hydrolysis is favored by heterogeneous reaction, high specific surface area or small Zn particles favor high $H_2$ production rates [12].

Melchior et al. prepared $H_2$ production by steam-hydrolysis of zinc vapor. The hydrolysis reactor consisted of a hot-wall tube containing a flow of Zn (g) that was steam-quenched to co-produce $H_2$ and Zn/ZnO nanoparticles. The effects of the reactor wall temperature on the Zn-to-ZnO chemical conversion and particle yield were examined. Solid products were characterized by X-ray diffraction, $N_2$ adsorption, and SEM microscopy. Here, surface reaction and coagulation dominated particle dynamics as observed in experimental runs with varying reaction zone temperatures downstream of the quench unit at a quenching flow rate of 20 l/min. As the reaction zone temperature was increased from 573 to 873 K, overall chemical conversion increased from 42% to 66%, mole fraction of ZnO particles for collected in the filter increased from 8% to 66%. At 873K, the maximum $H_2$ yield derived exclusively from hydrolysis of gas-borne particles collected in the filter was 22% $H_2$ [13].

2.6.2.2 Effect of Carrier Gas

Wegner et al. Synthesized zinc oxide nanoparticles and $H_2$ production by varying carrier gas flow rate. As the carrier gas flow rate was increased from 0.5 l/min to 1 l/min. Higher mass flow rates of the carrier gas resulted in lower $H_2$ concentration and small particle size. This can be explained by higher gas velocities and shorter times for Zn conversion with water [11].

Melchior et al. synthesized zinc oxide nanoparticles and $H_2$ production by varying carrier gas flow rate. Increasing carrier gas flow rate from 1 to7.5 l/min led to a decrease of the overall chemical conversion from 95% to about 65%, while a further increase to 25 l/min appeared to have no significant effect on of the overall chemical conversion. At carrier gas flow rate = 20 l/min and $T_{EZ}$ = 1148K, the major contribution to $H_2$ production derived from hydrolysis of Zn deposits on the reactor walls. For carrier gas flow rate < 7.5 l/min, less than 3% resulted from the collected samples on the filter. A maximum aerosol contribution of 9% was found for carrier gas flow rate = 20 l/min [13].

### *2.6.3 Hydrolysis of Zinc nanoparticles*

Funke et al. showed the hydrolysis of zinc powder in an aerosol to determine if high conversions were feasible at short residence time and high dispersion. Zinc particles with an average size of 158 nm were reacted with water vapor to form hydrogen and zinc oxide in an aerosol flow tube reactor at ambient pressure (82 kPa) and temperature between 653 and 813K with water concentration of 3%. The highest conversion observed in the flow system was about 24% at 813K and a gas residence time of 0.6 s. Non-isothermal thermogravimetric analysis (TGA) indicated that complete conversion of zinc to zinc oxide could be achieved for longer residence time. Activation energy of 132 kJ/mol was calculated from the TGA experiments using a model-free isoconversional method. Standard reaction models did not describe the data so an empirical order of reaction rate law was used instead. Reaction rates in the aerosol flow reactor were higher than those calculated from the TGA

measurements, likely due to lower mass and heat transfer resistances in the aerosol [14].

Frank et al. showed the hydrolysis rate of submicron Zn particles has measured by thermogravimetric analysis at 330–360 $^{o}$C and water vapor mole fractions y = 0.1–0.5 without oxygen. The temperature range was chosen carefully to avoid particle sintering during reaction and to be just below the Zn melting point which was desired for in-situ $H_2$ formation on suspended Zn particles. The hydrolysis rate of Zn particles was quantified by a core-shell model. The independence of Zn oxidation on oxidant composition showed that late Zn hydrolysis was limited by Zn diffusion. The measured activation energy was lower than that
reported in literature for bulk Zn oxidation. This indicated that, for the employed small Zn particles, the dissolution of Zn from the core into the shell might need less activation energy than from foils, discs, or other macroscopic materials traditionally used for kinetic analyses. By combining the measured rate laws and giving the appropriate transition conditions, a ready-to-use overall rate law was derived. The parabolic component of that reaction rate law was the slowest and might be the limiting one to determine reaction extent and required process residence time during $H_2$ production by the 2-step water-splitting cycle. On the other hand, if Zn particles were extremely small (e.g. less than 5 nm), the parabolic component of Zn hydrolysis might be avoided due to the large surface-to-volume ratio and consequently greatly reducing the process residence time and employed reactor size [15].

Zachariah et al. (2010) investigated the substrate-free hydrolysis of Zn nanocrystals. In this work, they combined two different ion-mobility schemes in series to study the hydrolysis kinetics of size-selected zinc nanocrystals (NCs). The first mobility characterization size selected particles with a differential mobility analyzer (DMA). The second mobility characterization employed an aerosol particle mass analyzer (APM) and measures changes in mass resulting from a controlled hydrolysis of the Zn NCs. A low temperature reaction mechanism was proposed to explain the mass change behavior of Zn NCs hydrolysis at 100–250 $^{o}$C. At low temperatures (below150 $^{o}$C) Zn NCs could react with water and generated solid zinc

hydroxide and released hydrogen gas. At higher temperatures, the zinc hydroxide decomposition reaction $Zn(OH)_2 \longrightarrow ZnO + H_2O$ started to compete with the hydrolysis reaction and form ZnO. This mechanism is consistent with the experiment observations and could produce hydrogen at the temperature range of about 100–150 $^oC$. Complete conversion of 70 nm Zn NC was achieved at 175 $^oC$ with the residence time of 10 s and water vapor mole fraction of 19%. An Arrhenius law was used to extract the reaction kinetic parameters. The activation energy of the hydrolysis reaction for 70 nm Zn NCs was determined to be 24 kJ/mol and the reaction order with respect to the water vapor mole fraction was found to be 0.9 [16].

### *2.6.4 Other Synthesis Methods*

Although the vapor transport process is the dominant synthesis method for growing semiconducting nanostructures such as ZnO, GaN and Si nanowires, other growth methods such as electrode position, sol-gel, polymer assisted growth have been developed in parallel. These methods provide the possibility of forming ZnO nanostructures at low temperature. For example, in an electrode position method, anodic aluminum oxide membrane (AAM) with highly ordered nanopores has been used as a template for the growth of zinc nanowires array via electrode position. Then the nanowire array can be oxidized at 300$^oC$ for 2 hours to obtain ZnO nanowire array [17]. In a sol-gel synthesis method, AAM has also been used as the template that was immersed into a suspension containing zinc acetate for 1 minute, then heated in air at 120$^oC$ for 6 hours. ZnO nanofibers were eventually obtained after removing the AAM template [18]. This sol-gel process was further improved by an electrochemical method in order to obtain nanorods with diameter smaller than 50 nm. These methods are complementary to the vapor transport synthesis of ZnO nanostructure, and also employ less severe synthesis conditions, which provide great potential for device application.

## 2.7 Condensation and Evaporation

The formation and growth of aerosol particles by condensation is the principal method of aerosol production in nature and is the most important mass-transfer process between the gas phase and the particulate phase. This process usually requires a supersaturated vapor and is initiated by the presence of small particles (nuclei) or ions that serve as sites for particle formation.

### *2.7.1 Homogeneous Nucleation*

Homogeneous nucleation is the formation of particles from a supersaturated vapor without the assistance of condensation nuclei or ion. The process is also call *self-nucleation*. This type of particle formation is rare for water vapor in the atmosphere, but it can be readily produced in the laboratory to study the process of formation and growth. Even in unsaturated vapor, the attractive forces between molecules, such as van derwaals forces, lead to the formation of molecular clusters. The clusters are formed continuously, but they are unstable and continuously disintegrate. When the vapor is supersaturated, the number concentration of clusters increases to the point where they collide with one another frequently. This process is similar to coagulation, except that the “agglomerates” disintegrate soon after being formed. The greater the supersaturation, the greater the number concentration of clusters and the more frequent is the formation of transient “agglomerates” having a size exceeds *d* (d* is Kelvin diameter).* Once such an “agglomerate” exceeds *d*,* even momentarily, it becomes stable and grows by condensation to form a large particle. For a given temperature, the supersaturation required for this event to happen occurs at a well-defined point called the *critical saturation ratio.* In photochemical smog formation, certain gas phase reactions are promoted by ultraviolet light and form low vapor-pressure reaction products. Because of their low vapor pressure, these products exist at high supersaturation and form particle by homogeneous nucleation. When an increase in aerosol mass concentration occurs in the atmosphere by this mechanism, it is called *gas-to-particle conversion.* Since a stable droplet is formed when the droplet diameter exceeds *d** for a particular saturation ratio. The droplet has

passed a threshold and will grow by condensation. The rate of growth depends on the saturation ratio, particle size and particle size relative to the gas mean free path. When a particle first starts to grow, its size will likely be less than the mean free path. For this condition, the rate of particle growth is governed by the rate of random collisions between the particle and the vapor molecules. For particles larger than the gas mean free path, the growth depends, not on the rate of random molecule collisions, but on the rate of diffusion of molecules to the droplet surface.

### *2.7.2 Heterogeneous Nucleation*

Heterogeneous nucleation or nucleated condensation is a process of particle formation and growth that is promoted by the presence of condensation nuclei or ions. Whereas the homogeneous nucleation usually requires saturation ratio of 2-10, the heterogeneous nucleation can occur at supersaturations of only a few percent. Insoluble nuclei can provide a passive site for the condensation of supersaturated vapor. At a given level of supersaturation, an insoluble nucleus with awetable surface will have an adsorbed layer of vapor molecules on its surface. If its diameter is greater than $d^*$, the nucleus will behave like a droplet of that size and grow by condensation. However, the actual situation is more complicated because ability of particle to nucleate condensation depends on many factors, including its size, shape, chemical composition, surface structure and surface charge.

# CHAPTER III

## EXPERIMENTAL

The synthesis of zinc oxide nanoparticles and $H_2$ production by Hydrolysis of zinc vapor process using zinc foil as source material is explained in this chapter. The chemicals, samples preparation and characterization techniques are also explained.

### 3.1 Raw Material

Zinc foils as shown in Figure 3.1, which were used as raw materials for the synthesis of ZnO and $H_2$ in this research, were obtained from Univenture Co., Ltd. The purity of zinc is higher than 99.995%.

**Figure 3.1** Zinc foils as raw material.

### 3.2 Experimental Procedures

ZnO nanoparticles and $H_2$ are synthesized from the reaction between zinc vapor, evaporated from zinc foil, and steam supplied to the reactor without the presence of catalyst. The system was consisted of a ceramic tube reactor (120 cm in length, 6.2 cm in the outer diameter) placed inside a horizontal tube furnace, as shown in Figure3.2. The number of smaller ceramic tubes (10 cm in length, 4.8 cm in the outer diameter) was placed inside the ceramic tube reactor to collect particle deposited within the system. Steam was generated in separated vessel and thermometer is controlled the temperature, as shown in Figure 3.3.One end of the ceramic tube was connected to gas inlets and the other end was connected to a rotary vacuum pump through a series of product collecting means, i.e., a dry chamber, a wet chamber and filters cold trap respectively, as shown in Figure 3.4–3.6.

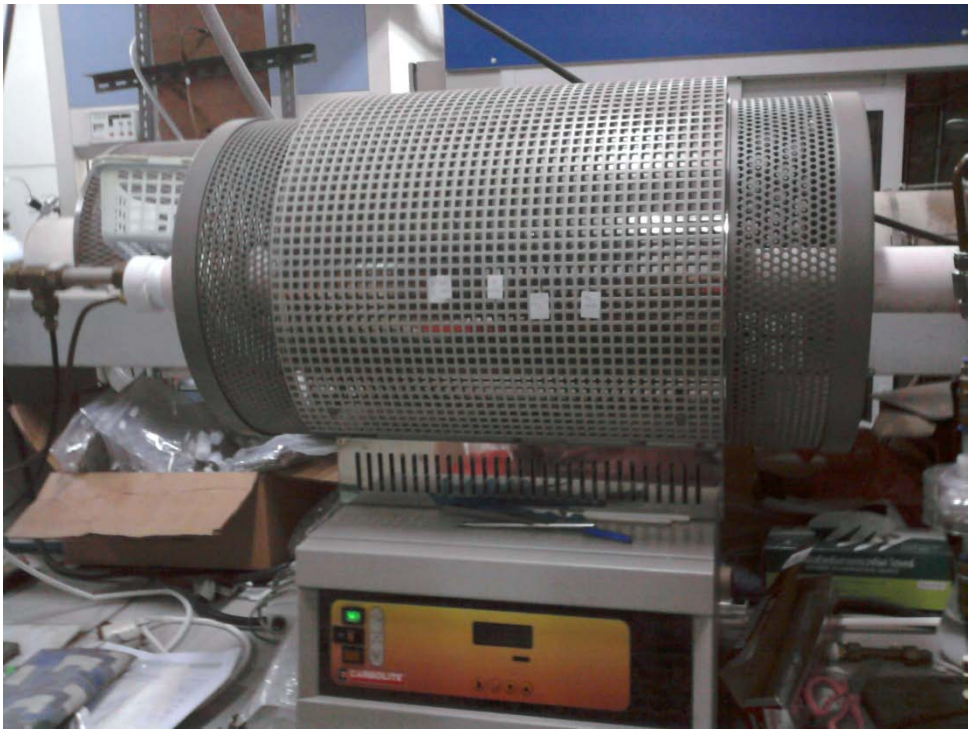

**Figure 3.2** A horizontal tube furnace and a ceramic tube reactor

**Figure 3.3** A steam generator

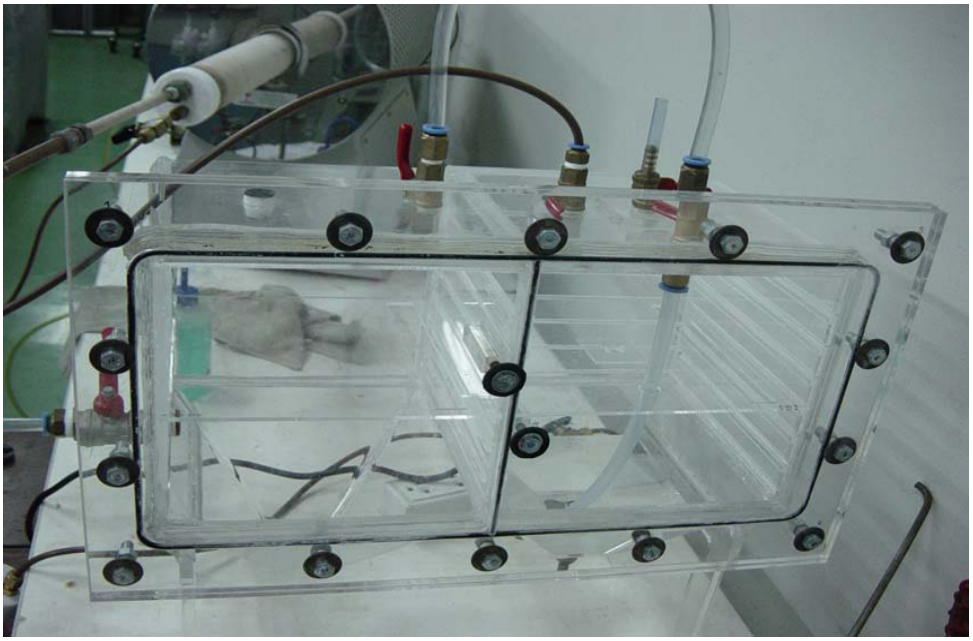

**Figure 3.4** Dry chamber and wet chamber for collecting the product coming out from the reactor

**Figure 3.5** Two filter holders installed at the outlet of the collecting chamber.

**Figure 3.6** A cold trap

The whole system is shown in Figure 3.7. For each experiment, about 3.1 g of zinc foils were wrapped on ceramic tube at evaporation zone and argon is carried in to reaction zone. Steam was fed co-currently with the zinc vapor into the reaction zone by argon. Then the reactor was evacuated to the low pressure by vacuum pump and subsequently filled with argon gas back to 1 atm repeat until the reactor no oxygen gas (check by GC) before heating up to desired temperature. Nitrogen gas was also continuously supplied to the reactor during the heat up process. When the furnace reached the desired temperature, steam was supplied to the reactor to initiate the reaction. The flow rate of both nitrogen and argon were controlled by flow meters. The pressure within the system was kept at 1 atm by means of the vacuum pump. Solid products collected by filter downstream were characterized by XRD SEM and ICP, while the gas was periodically sampled and analyzed by GC. After 1 h, the steam supply was cut off and the furnace was cooled down to room temperature.

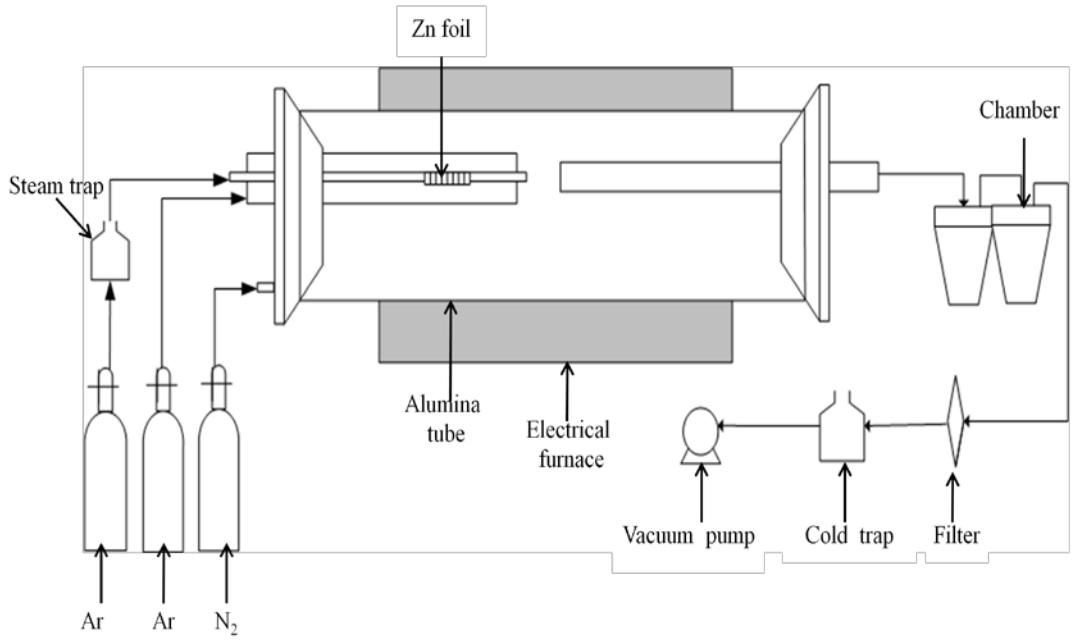


**Figure 3.7** Schematic diagram for the experimental set up.

The investigation of this work was separated into 4 parts as follow.

### *3.2.1 The Effect of Evaporation Temperature*

In this part, the effects of zinc evaporation temperature on morphology and particles size of the synthesized ZnO , % yield of $H_2$ gas product and % weight of ZnO in the filter were studied. Therefore, the evaporation temperature of the tube furnace used for the synthesis of ZnO nanoparticles and $H_2$ gas was varied from 600, 650, 700, 800 and 850 $^oC$. Nitrogen gas flow rate, zinc vapor flow rate and steam flow rate were kept constant at 1 l/min, 1.5 l/min and 05 l/min, respectively. Reaction temperature were kept constant at 750 $^oC$

### *3.2.2 The Effect of Zinc vapor Flow Rate*

In this part, the effect of zinc vapor flow rate on morphology and particles size of the synthesized ZnO , % yield of $H_2$ gas product and % weight of ZnO in the filter were studied. Therefore, zinc vapor flow rate was varied from 0.5, 1 and 1.5 l/min. For this set of experiment, the zinc evaporation temperature was fixed at 850$^oC$, reaction temperature was fixed at 750$^oC$ and 900 $^oC$, nitrogen gas flow rate and steam flow rate was kept at 1 and 0.5 l/min respectively.

### *3.2.3 The Effect of Reaction Temperature*

In this part, the effects of reaction temperature on morphology and particles size of the synthesized ZnO , % yield of $H_2$ gas product and % weight of ZnO in the filter were studied. Therefore, the reaction temperature of the tube furnace used for the synthesis of ZnO nanoparticles and $H_2$ gas was varied from 500, 600, 700, 800 850 and 900 $^oC$. Evaporation temperature was fixed at 850 $^oC$, nitrogen gas flow rate, zinc vapor flow rate and steam flow rate were kept constant at 1 l/min, 1.5 l/min and 0.5 l/min respectively.

### *3.2.4 The Effect of Resident Time*

In this part, the effects of reaction time were studied by varying the distant from inlet tube and outlet tube at 1, 2, 3 and 4 cm respectively. Evaporation temperature was fixed at 850 $^{o}$C, reaction temperature was fixed at 900 $^{o}$C nitrogen gas flow rate, zinc vapor flow rate and steam flow rate were kept constant at 1 l/min, 0.5 l/min and 0.5 l/min respectively.

## 3.3 Sample Characterization

The instruments used to characterize properties of the particle included Scanning Electron Microscope (SEM) model Hitachi S-3400N, X-ray Diffractometer (XRD) model SIEMENS D5000 and Inductive Coupled Plasma Optical Emission Spectrometer (ICP-OES) . The instruments used to characterize gas product is Gas Chromatography( GC) model Shimadzu GC-8A.

.

### *3.3.1 Scanning Electron Microscopy (SEM)*

Morphology and size of the particle were observed by using SEM at a research laboratory collaborated between Mektec Manufacturing Corporation (Thailand) Ltd and Chulalongkorn University. SEM specimens were prepared by taking the powder on SEM substrate, and then directly placing the piece onto a conductive platinum coated microscope grid. The specimens were loaded into a sample chamber, and observations were immediately started using image catcher scanner for taking the photos. A photo of the scanning electron microscopy machine is shown in Figure 3.6.


**Figure 3.6** Scanning Electron Microscope (SEM).

### *3.3.2 X-Ray Diffraction (XRD)*

X-ray diffraction (XRD) analysis of particle was performed by a SIEMENS D5000 diffractometer at the Center of Excellence on Catalysis and Catalytic Reaction Engineering, Chulalongkorn University as shown in Figure 3.7. The X-ray diffractometer was connected to a personal computer with Diffract AT version 3.3 program. The particle was spreaded on the slide and then set in the equipment which provide X-ray beam for the analysis. The measurement was carried out by using CuKα radiation with Ni filter. The condition of the measurement is shown as followed:

2θ range of detection : 20 – 80 °
Resolution : 0.04 °
Number of Scan : 15.


**Figure 3.7** X-Ray Diffraction (XRD).

### *3.3.3 Gas Chromatography*

| Shimadzu GC-8A | |
|---|---|
| Detector | TCDGC8A |
| column | Molecular sieve |
| carrier gas | Ar |
| flow carrier gas | 40 ml/min |
| Temp | $^{o}$C |
| injector | 100 |
| column | 70 |
| detector | 70 |


**Figure 3.10** Gas chromatography (GC)

### *3.3.4 Inductive Coupled Plasma Optical Emission Spectrometer (ICP-OES)*

The actual amount of the metals loading were determined by a Perkin Elmer Optima 2100DV AS93 PLUS inductive coupled plasma optical emission spectrometer.

# CHAPTER IV

## RESULTS AND DISCUSSION

The aim of this research is to find optimal condition for synthesis ZnO nanaparticle and $H_2$ gas product from hydrolysis of zinc vapor process. The effects of evaporation temperature, zinc vapor flow rate, reaction temperature and reaction time were investigated.

Tube furnace reactor was used in this research. The inside reactor was not temperature constant, as shown in Figure 4.1

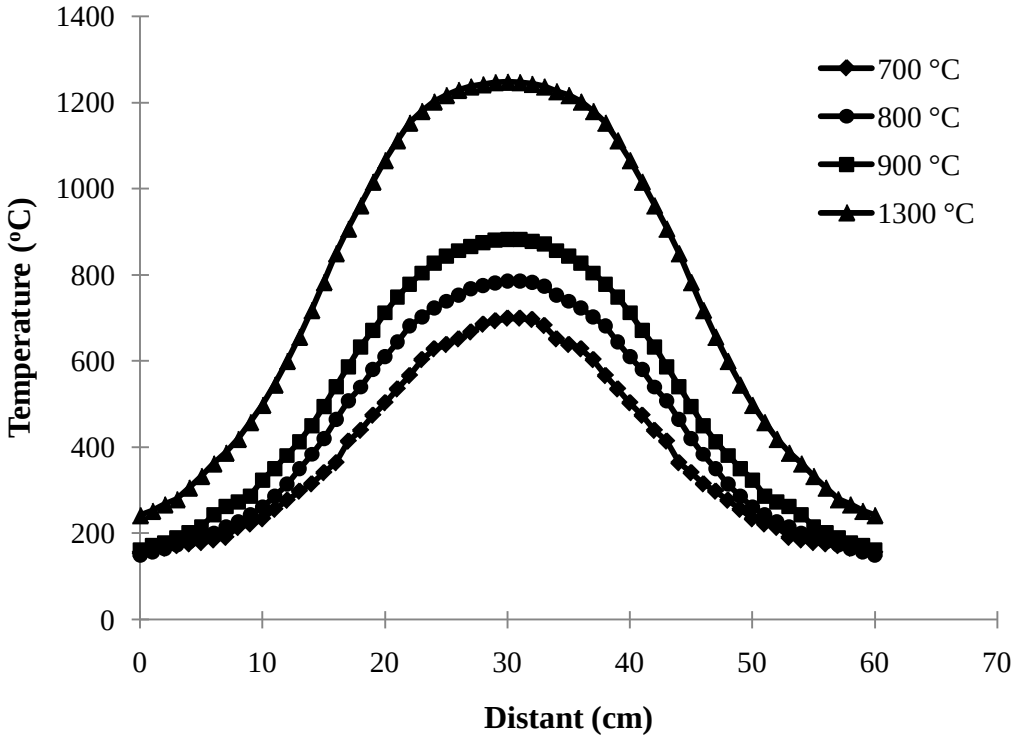


**Figure 4.1** Temperature profiles inside the reactor.

## 4.1 Effect of Evaporation Temperature

Effect of concentration of zinc vapor was studied by varying the evaporation temperature of zinc from 600, 650, 700, 800 and 850 $^{o}$C. Flow rate of nitrogen gas, carrier gas for zinc vapor and supplied steam were kept constant at 1, 1.5 and 0.5 l/min, respectively. Reaction temperature was kept constant at 700 $^{o}$C.

In this section, the experimental-setup is shown in Figure 4.2. For all experiments, the positions of all alumina tubes were fixed and the temperature at the center of the reactor was fixed at 850 $^{o}$C. The evaporation temperature of zinc was varied by changing the position where zinc foil was located.

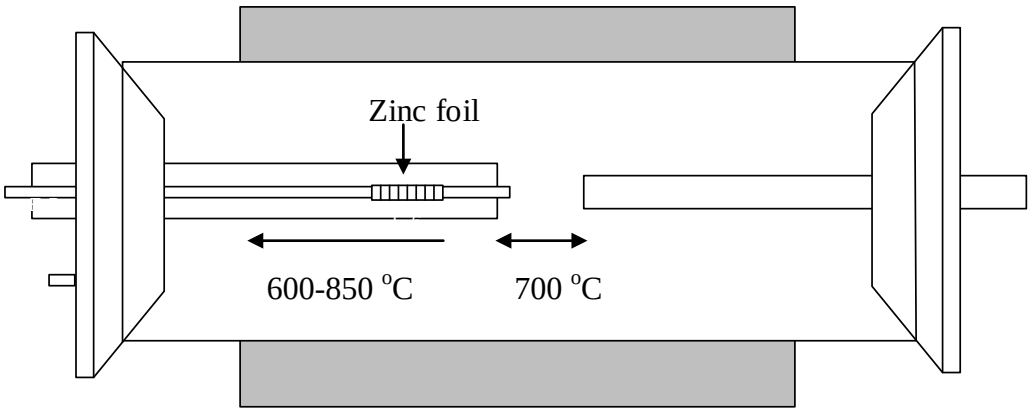


**Figure 4.2** Experimental-setup for the studies of the effect of zinc evaporation temperature.

Figure 4.3 shows rates of $H_2$ production with respect to time. Report of $H_2$ gas was started when the set point temperature was reached (reaction of time 0 min). It should be noted that $H_2$ production was found at the reaction time of 0 min because the supplied steam was fed to reactor before the temperature had reached the set point. From Figure 4.3, patterns of $H_2$ production using evaporating temperature of 800 and 850 $^{o}$C, were similar. During the reaction time of 0-10 min, $H_2$ production rate increased because in this period concentration of Zn vapor was increased. At the reaction time 15 min the value of the $H_2$ production rate reached the highest, and after which amount of zinc foil was decreased. Once the concentration of zinc vapor was decreased, the reaction between zinc vapor and supplied steam decreased, leading to decreased production of $H_2$. At the evaporating temperature of 600 and 650 $^{o}$C, the $H_2$ production rate was increased with increasing the reaction time and the $H_2$ production rate became constant after 30 min until the experiments were finished (60 min) because Zn foil hardly evaporated at this temperature. For the evaporating temperature of 700 $^{o}$C, $H_2$ production rate became constant after 20 min to 35 min. Therefore, after 35 min $H_2$ production rate was decreased because amount of zinc foil was decreased.

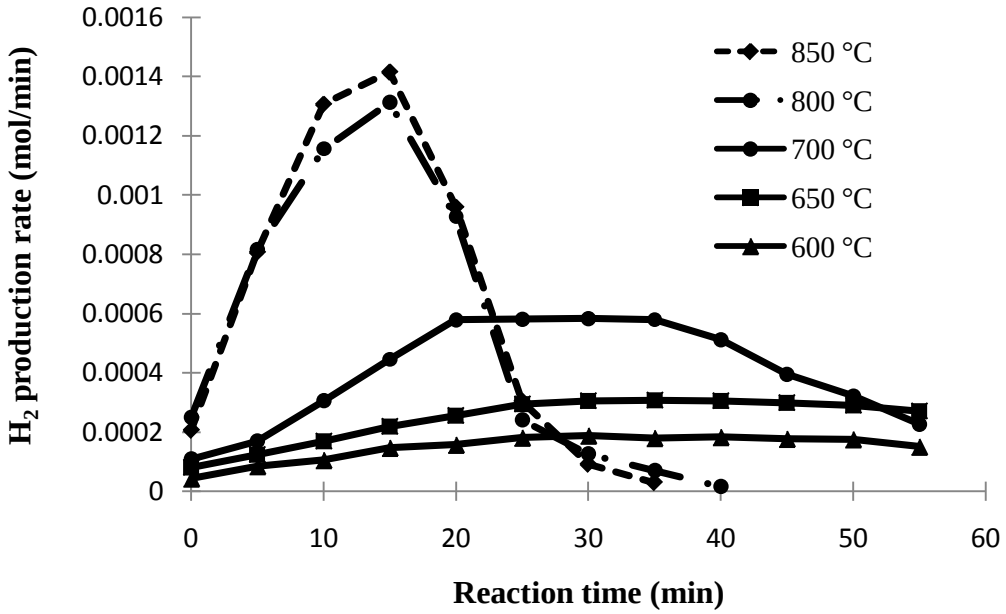


**Figure 4.3** Rate of $H_2$ production with respect to reaction time, using various evaporation temperature of zinc. Flow rates of nitrogen gas, zinc vapor and supplied steam were kept constant at 1, 1.5 and 0.5 l/min, respectively. Reaction temperature was kept constant at 700 $^{o}$C.

In this research, the $H_2$ yield was determined with respect to the evaporated Zn as

$$\text{Actual } H_2 \text{ yield / theoretical yield} = \frac{\text{moles of } H_{2,GC}}{\text{moles of } H_{2,max}}$$

Where $H_{2,GC}$ refers to the amount of $H_2$ produced (based on the concentration measured by GC integrated over the duration of an experiment), and $H_{2,max}$ refer to the theoretical maximum amount of $H_2$ that could have been produced under the assumption of complete hydrolysis of the evaporated zinc.

Figure 4.4 shows $H_2$ yield as function evaporation temperature. Five values of zinc evaporation temperature investigated were 600, 650, 700, 800 and 850 $^oC$, respectively. It was found that, as the evaporation temperature was increased, the actual yield of $H_2$ gas was increased. This can be explained by high concentration of zinc vapor when high evaporation temperature was used, resulting in more aggressive reaction. Moreover, when the evaporation temperature was higher than the reaction temperature (700 $^oC$), Zn vapor could condense in to Zn particles. Therefore, the hydrolysis reaction was occurred in both homogeneous phase and heterogeneous phase. When evaporation temperature was increased, resulting in higher concentration of Zn vapor. It was more potential than Zn vapor could condense in to Zn particles when increasing evaporation temperature. So $H_2$ yield of evaporation temperature of 850 $^oC$ was higher than that at 800 $^oC$. The highest yield of $H_2$ gas obtained was 51.19 % at the evaporation temperature of 850 $^oC$.

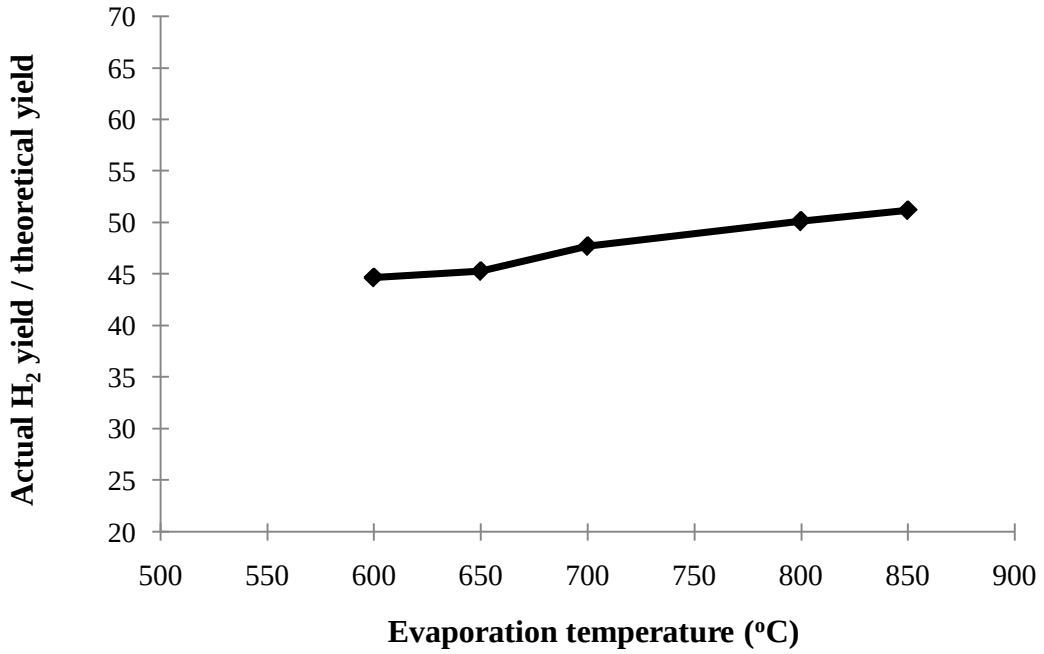


**Figure 4.4** Yield of $H_2$ (yield actual/yield theoretical) as function of zinc evaporation temperature investigated were 600, 650, 700, 800 and 850 $^oC$, respectively. Flow rates of nitrogen gas, zinc vapor and supplied steam were kept constant at 1, 1.5 and 0.5 l/min, respectively. Reaction temperature was kept constant at 700 $^oC$.

Figure 4.5 shows the XRD patterns of particles collected in the filter, when the evaporation temperature was, 700, 800 and 850 $^{o}$C respectively. All XRD patterns can be indexed to mixture between hexagonal wurtzite structure of ZnO and unreacted Zn. No diffraction peak corresponding to other impurity phases was found in any sample.

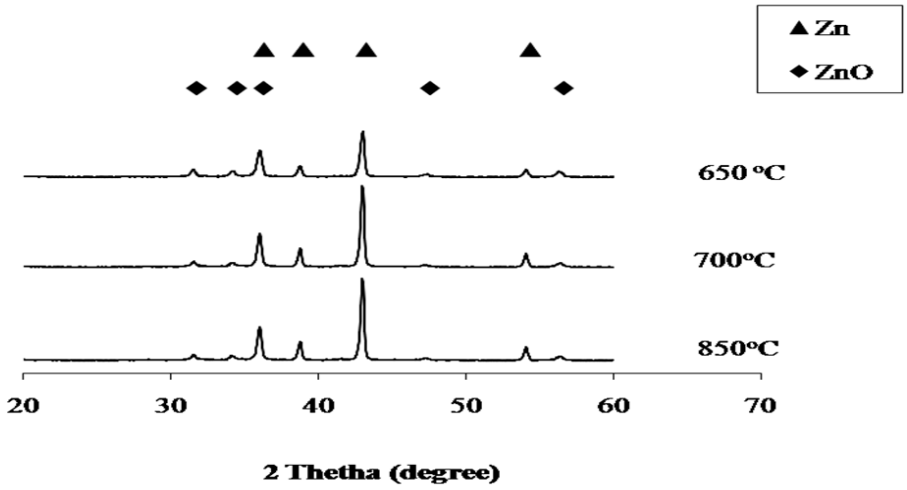


**Figure 4.5** XRD patterns of products collected by filter from the reaction using zinc evaporation temperature of 650, 700 and 850 $^{o}$C. Flow rates of nitrogen gas, zinc vapor and supplied steam were kept constant at 1, 1.5 and 0.5 l/min, respectively. Reaction temperature was kept constant at 700 $^{o}$C.

Figure 4.6 shows fraction of ZnO (mole %) in the product collected by the filter as function evaporation temperature. The fraction of ZnO was determined by ICP. It was found that the evaporation temperature was increased, the fraction of ZnO within the collected product was increased as well. The highest fraction of ZnO obtained was 24.66% mole at the evaporation temperature of 850 $^{o}$C.

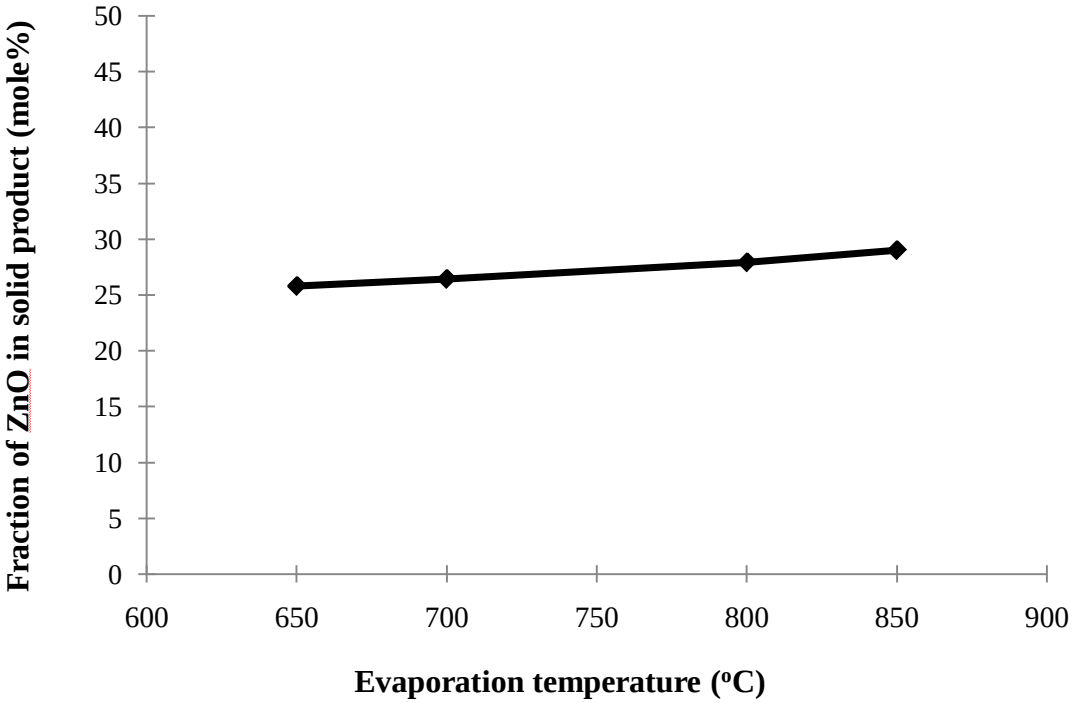


**Figure 4.6** Fraction of ZnO (mole %) in the product collected by the filter as function of evaporation temperature. Flow rates of nitrogen gas, zinc vapor and supplied steam were kept constant at 1, 1.5 and 0.5 l/min, respectively. Reaction temperature was kept constant at 700 $^{o}$C.

Figure 4.7 shows micrographs of products collected by filter when zinc evaporation temperature was varied from 600 to 850 $_{o}$C. It was found that particles collected in all experiments were hexagonal in shape but nonuniform in size. Besides, they were agglomerated. When the evaporation temperature was low, the particles were small as shown in Figure 4.6a. However, when the evaporation temperature was increased to 850 $^{o}$C, the particles became larger. This can be explained that, at high evaporation temperature, zinc vapor was introduced to the reaction zone at high concentration (high zinc nuclei), since the flow rate of its carrier gas was kept constant, leading to high reaction rate. The ZnO product was generated slowly in low concentration, therefore the size became small. As agreed with H. H. Funke et al [13] and F. O. Ernst et al [14]. Average diameters of the particulate product were measured

by an image processing program (SemAfore 4.0), based on 50 randomly selected particles from SEM images. It was found that when the evaporation temperature was increased, the average diameter of the particulate product was increased. The average diameters of the particulate product were 210, 281, 306 and 312 nm where the evaporation temperature was 650, 700, 800 and 850 $^{o}$C, respectively.

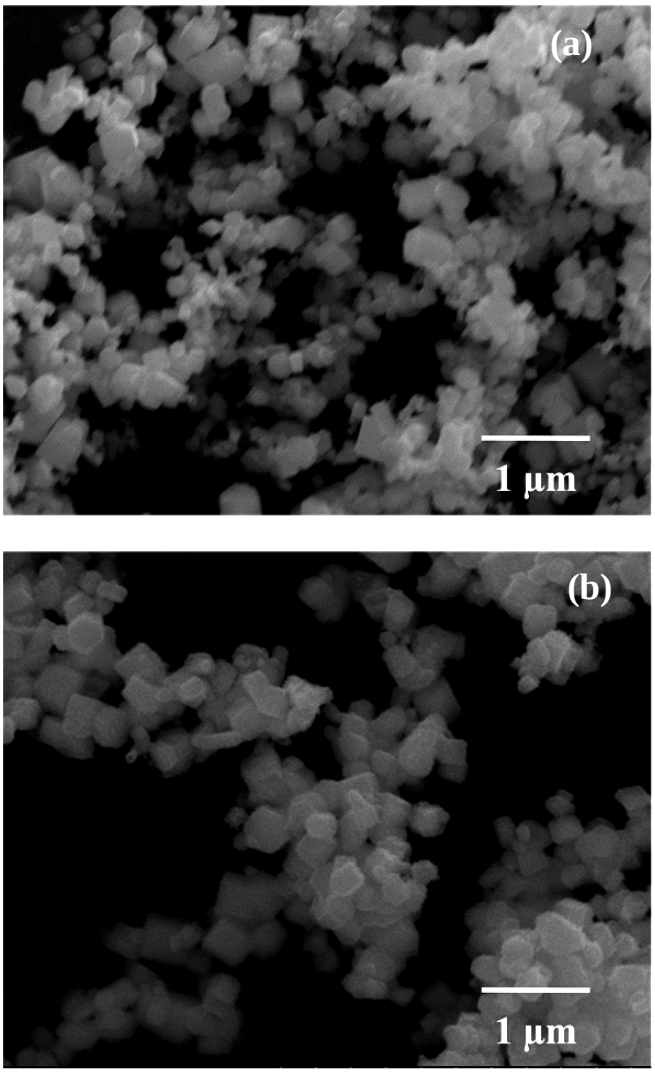


**Figure 4.7** SEM micrographs of products collected by filter when zinc evaporation temperature was 650 $^{o}$C (a), 700 $^{o}$C (b), 800 $^{o}$C (c) and 850 $^{o}$C (d). Flow rates of nitrogen gas, zinc vapor and supplied steam were kept constant at 1, 1.5 and 0.5 l/min, respectively. Reaction temperature was kept constant at 700 $^{o}$C.

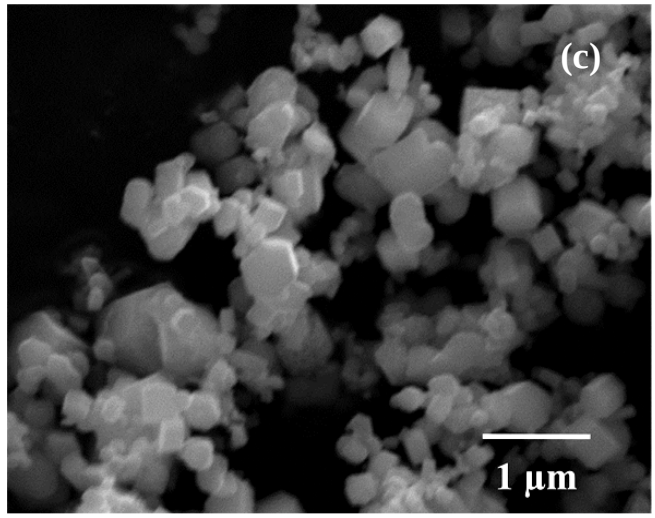


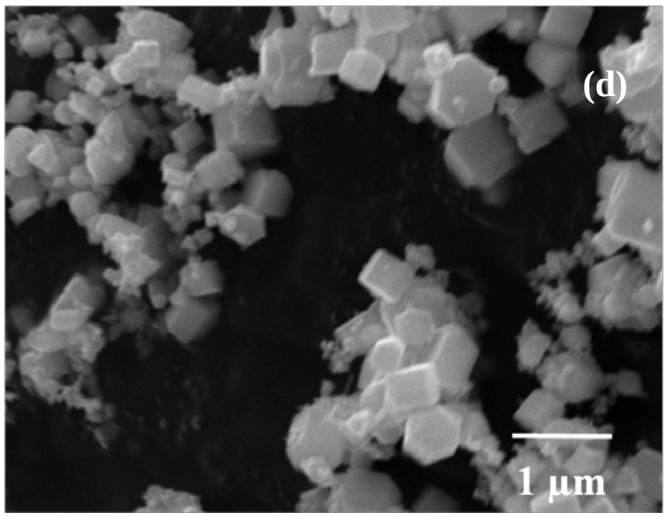


Figure 4.7 (continued)

The amounts of product collected at different positions of the system are shown in Table 4.1. It can be seen that the amount of product collected at every location increased with the increasing evaporation temperature because more zinc vapor was generated at higher temperature, and consequently the more ZnO product was formed and deposited in all parts of the reactor. In addition, this result can also support the earlier presumption that higher evaporation temperature due to the high zinc vapor concentration. Zinc nuclei could more occur.

**Table 4.1** The amount of products collected at each position of the system from the reaction with different value of zinc evaporation temperature.

| **Zinc evaporation temperature (˚C)** | **Amount of solid product collected** | | | | |
|---|---|---|---|---|---|
| | **Reaction zone (g)** | **Outlet zone (g)** | **Collecting system (g)** | **Filter (g)** | **Total (g)** |
| 650 | 0.102 | 0.013 | 0.135 | 1.175 | 1.425 |
| 700 | 0.144 | 0.021 | 0.272 | 2.583 | 3.020 |
| 800 | 0.275 | 0.098 | 0.835 | 1.889 | 3.097 |
| 850 | 0.364 | 0.110 | 1.306 | 1.215 | 2.995 |

## 4.2 Effect of Flow Rate of Zinc Vapor

The effect of zinc vapor flow rate was studied by varying flow rate of carrier gas (Ar) from 0.5, 1 and 1.5 l/min. For this set of experiment, the zinc evaporation temperature was fixed at 850 $^{o}$C. The reaction temperature was fixed at 700 $^{o}$C. Flow rates of nitrogen gas and supplied steam were kept at 1 and 0.5 l/min, respectively as shown in Figure 4.7.

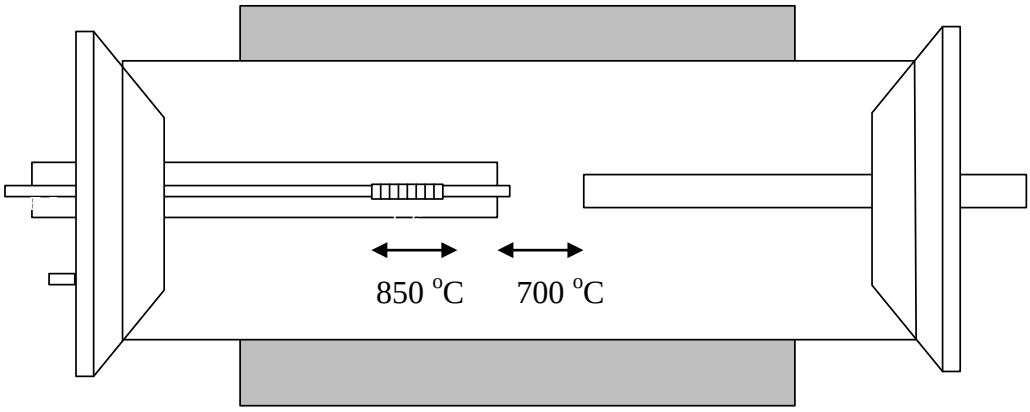


**Figure 4.8** Experimental-setup for the studies of the effect of flow rate of zinc vapor.

Figure 4.9 shows rate of $H_2$ production as a function of time for three different flow rate of Ar carrier gas for zinc vapor (0.5, 1 and 1.5 l/min). It was found that as the flow rate of carrier gas for zinc vapor was increased, the reaction time which yielded the highest $H_2$ production rate decreased. It is suggested that when the flow rate of the carrier gas for zinc vapor was increased, the rate of evaporation of zinc foil were increased. Because the higher flow rate of carrier gas can be carried zinc vapor out of evaporation zone faster. So low concentration of zinc vapor this zone due to zinc foil was evaporated to fast. However, since the amount of zinc foil put in to the reactor was the same for all experiments, this evaporation rate resulted in fast consumption of zinc foil. That is why $H_2$ production diminished faster when the Ar flow rate of 1.5 l/min was used. Yield of $H_2$ gas and fraction of ZnO in the product collected by the filter are shown in Figure 4.9.

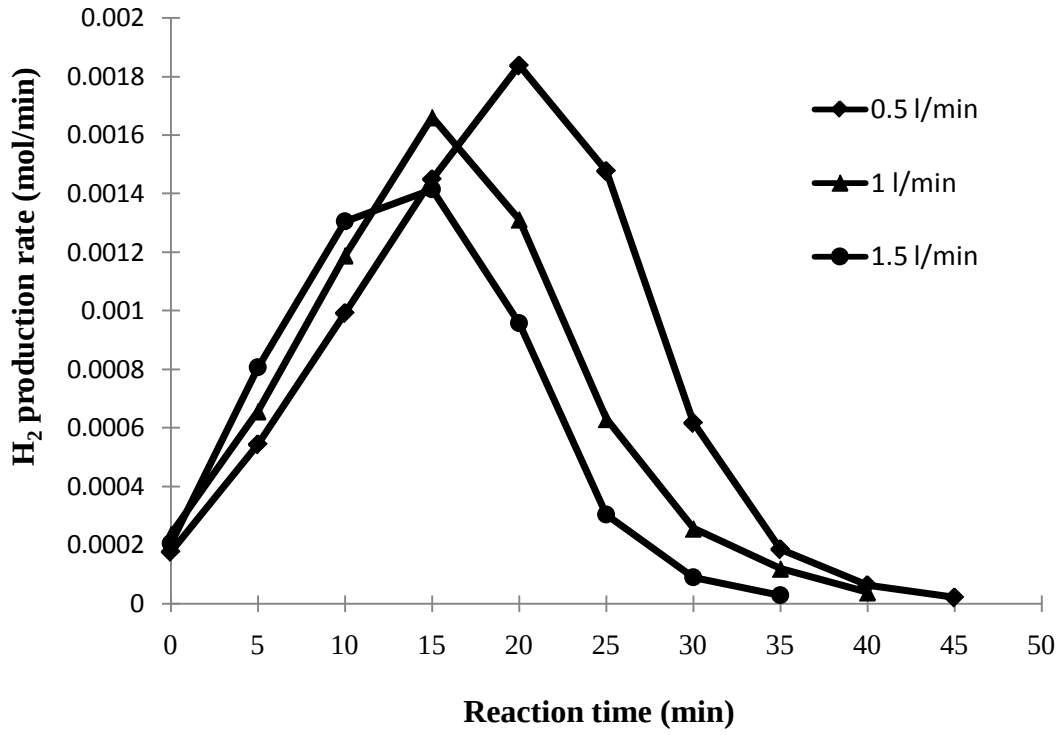


**Figure 4.9** Rate of $H_2$ production with respect to reaction time, using flow rate of the carrier gas (Ar) for zinc vapor of 0.5, 1 and 1.5 l/min. For this set of experiment, the zinc evaporation temperature was fixed at 850 $^{o}$C. The reaction temperature was fixed at 700 $^{o}$C. Flow rate of nitrogen gas and supplied steam was kept at 1 and 0.5 l/min, respectively.

The change in the flow rate of the carrier gas effects residence time, which is a period of time that reaction occur (mostly in the reaction zone), and the concentration of the zinc vapor in the system. By applying the higher flow rate, the residence time should be shorter as shown in Figure 4.10.

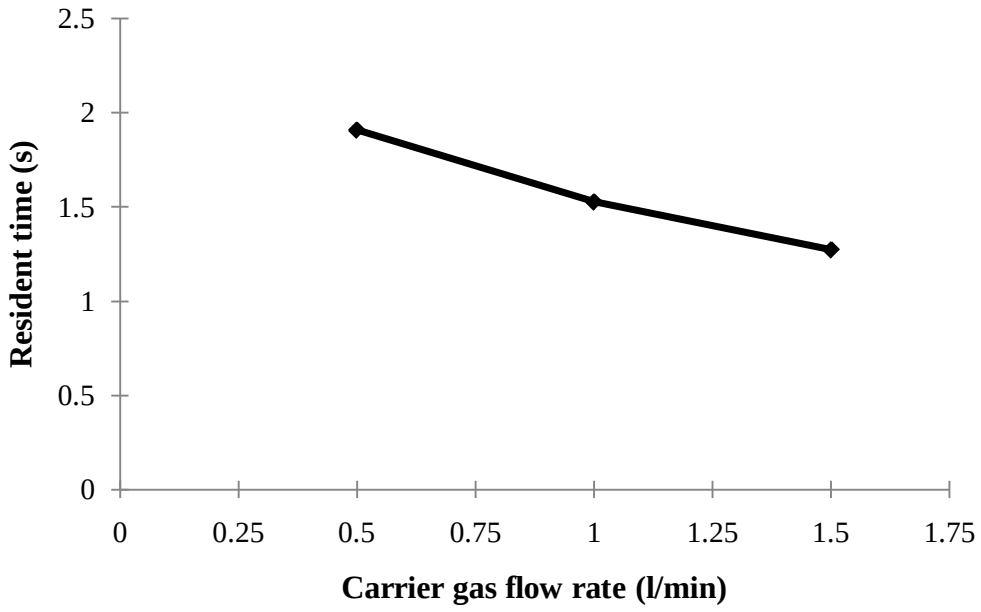


**Figure 4.10** Resident time of the reaction for this set of experiment, the zinc evaporation temperature was fixed at 850 $^{o}$C. The reaction temperature was fixed at 700 $^{o}$C. Flow rate of nitrogen gas and supplied steam was kept at 1 and 0.5 l/min, respectively.

From Figure 4.11, when the flow rate of the carrier gas for zinc vapor was increased, yield of $H_2$ gas decreased because the higher flow rate of the carrier gas provided shorter residence time of zinc vapor the system. This means that zinc and steam had less time to react to each other in the reaction zone. The highest of $H_2$ yield was 66 % when the Zn vapor flow rate was 0.5 l/min. Moreover, when the flow rate of the carrier gas for zinc vapor was increased, it resulted in increasing fraction of ZnO in the collected solid product. This can be explained that ZnO product formed in to large particles and deposited on the reactor wall. When the carrier gas flow rate was low, ZnO product could not be carried out of the reactor but for high carrier gas flow rate, ZnO product could be carried out of the reactor and collected by filter. It could be confirmed from micrographs of products in Figure 4.12. The highest of fraction of ZnO was 24.66 % mole when the Zn vapor flow rate was 1.5 l/min.

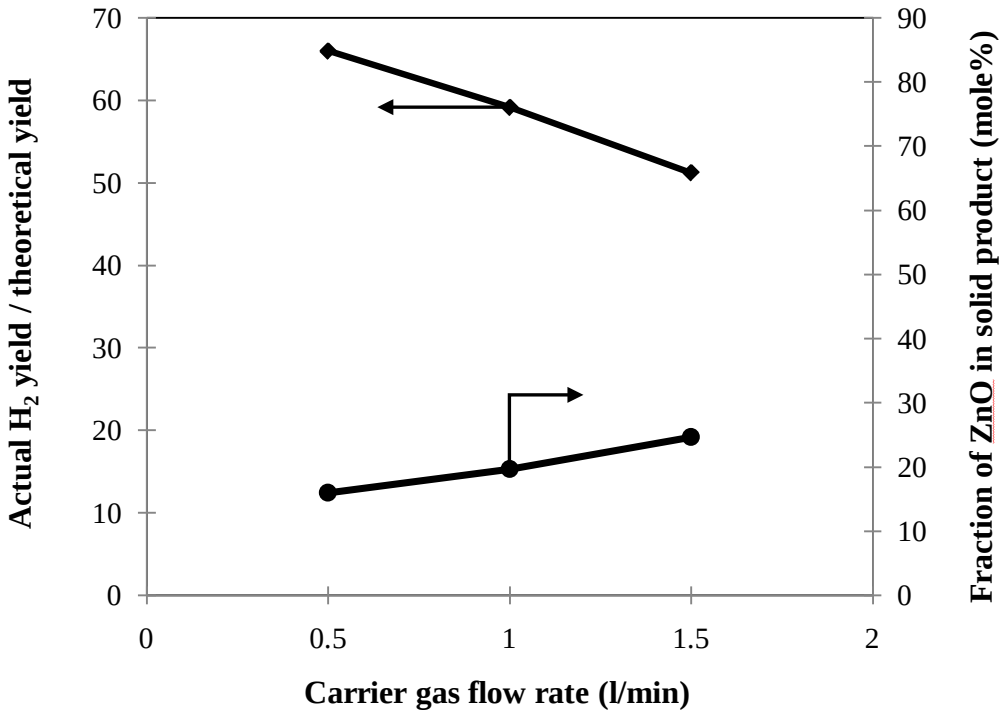


**Figure 4.11** Actual $H_2$ yield / theoretical yield and fraction of ZnO (mole %) in the product collected by the filter as function of Zn vapor flow rate. For this set of experiment, the zinc evaporation temperature was fixed at 850 $^{o}$C. The reaction temperature was fixed at 700 $^{o}$C. Flow rate of nitrogen gas and supplied steam was kept at 1 and 0.5 l/min, respectively.

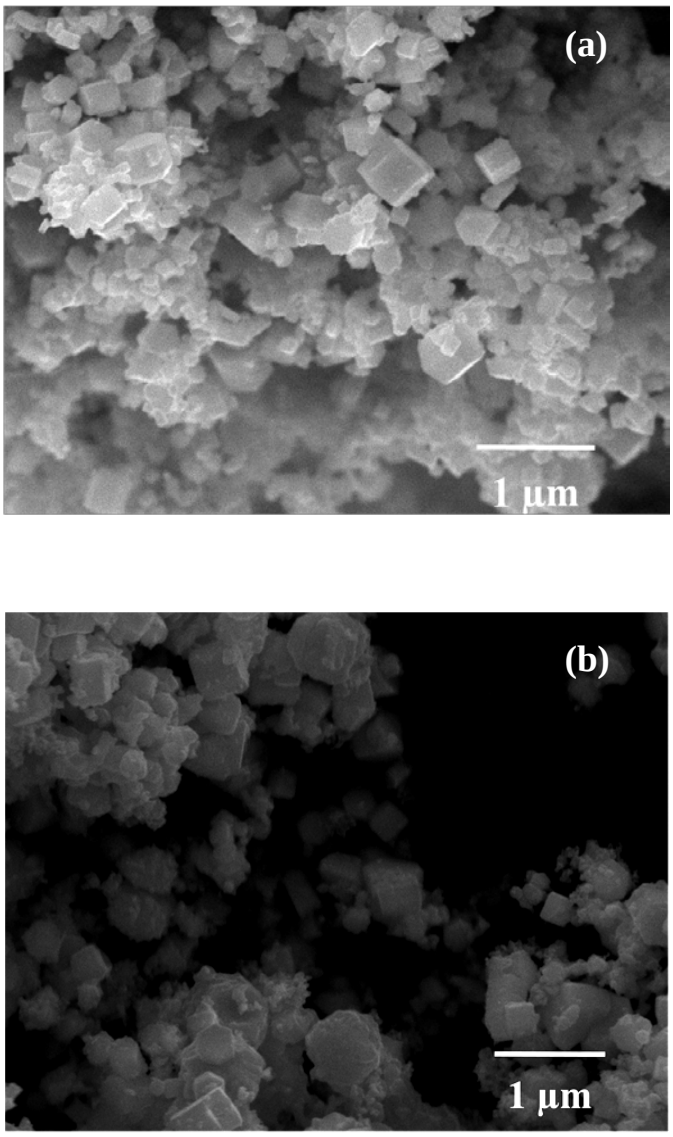


**Figure 4.12** SEM micrographs of products collected by filter when Zn vapor flow rate was 0.5 l/min (a), 1 l/min (b) and 1.5 l/min. For this set of experiment, the zinc evaporation temperature was fixed at 850 $^{o}$C. The reaction temperature was fixed at 700 $^{o}$C. Flow rate of nitrogen gas and supplied steam was kept at 1 and 0.5 l/min, respectively.

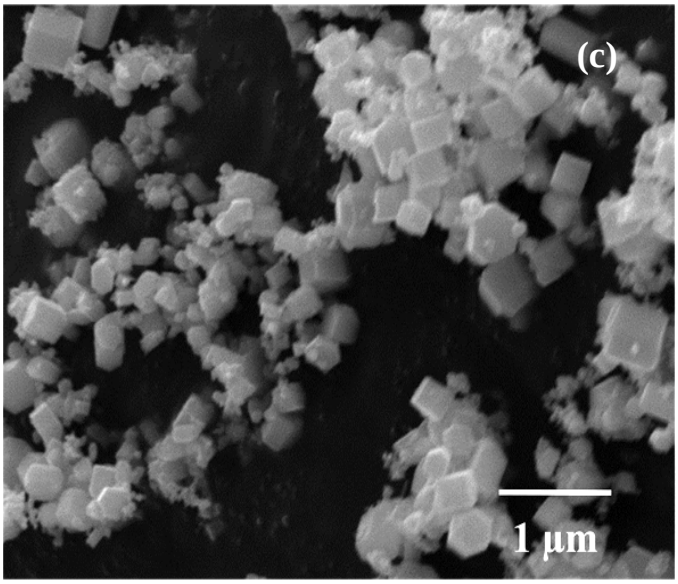


Figure 4.12 (continued)

Figure 4.12 shows micrographs of products collected by filter. It can be clearly observed that lower Zn vapor flow rate resulted in with larger size of particles product. Average diameters of the particulate product were measured by an image processing program (SemAfore 4.0), based on 50 randomly selected particles from SEM images. It was found that when the Zn vapor flow rate was increased, the average diameter of the particulate product was increased. The average diameters of the particulate product were 233, 267 and 312 nm where the Zn vapor flow rate was 0.5, 1 and 1.5 l/min, respectively.

Moreover, amounts of product collected at different positions of the system are shown in Table 4.2. It can be noticed that the higher flow rate brought more ZnO product into the collecting system. The residence time and the higher zinc vapor concentration should be the factor influencing this result as occurred in the previous results.

Table 4.2 The amount of the product collected at each position of the system from the reaction with different value of zinc carrier gas flow rate.

| **Flow rate of carrier gas for zinc vapor (mol/min)** | **Amount of solid product collected** | | | | |
|---|---|---|---|---|---|
| | **Reaction zone (g)** | **Outlet zone (g)** | **Collecting system (g)** | **Filter (g)** | **Total (g)** |
| 0.5 | 0.647 | 0.479 | 1.021 | 0.810 | 2.957 |
| 1 | 0.516 | 0.229 | 1.134 | 1.194 | 3.073 |
| 1.5 | 0.364 | 0.110 | 1.306 | 1.215 | 2.995 |

### 4.3 Effect of Reaction Temperature

To investigate effect of reaction temperature, the temperature was varied from 500, 600, 700, 800, 850, 900 and 1200 $^{o}$C. The evaporation temperature was fixed at 850 $^{o}$C, while the flow rates of nitrogen gas, zinc vapor and supplied steam were 1, 1.5 and 0.5 l/min, respectively.

In this section, the experimental-setup is shown in Figure 4.13. For all experiments, the position of zinc foil was fixed at 850 $^{o}$C. The positions of all alumina tubes were adjusted to achieve the desired temperature for the reaction zone.

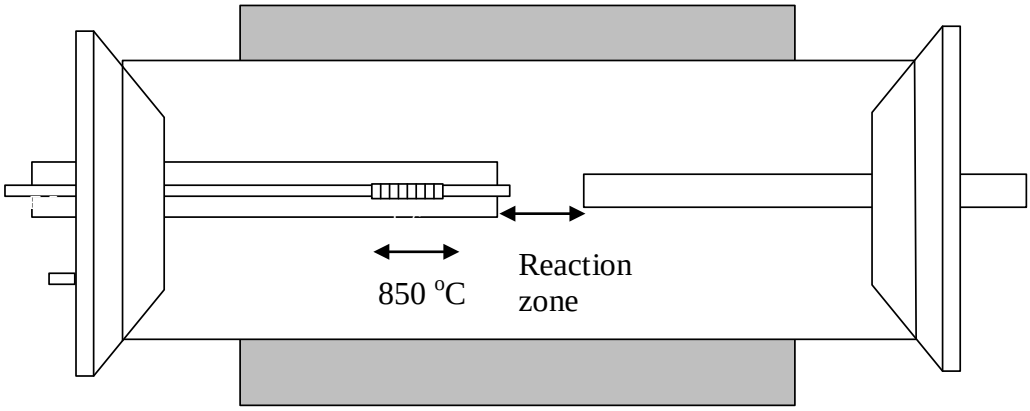


**Figure 4.13** Experimental-setup for the studies of the effect of reaction temperature.

.

Figure 4.14 shows rate of $H_2$ gas production with respect to reaction time, using reaction temperature in the range of 500 to 1200 $^oC$. It was found that from all experiments, the highest $H_2$ production rate was achieved at 15 min and not found $H_2$ production at 40 min because the total flow rate in the system became constant.

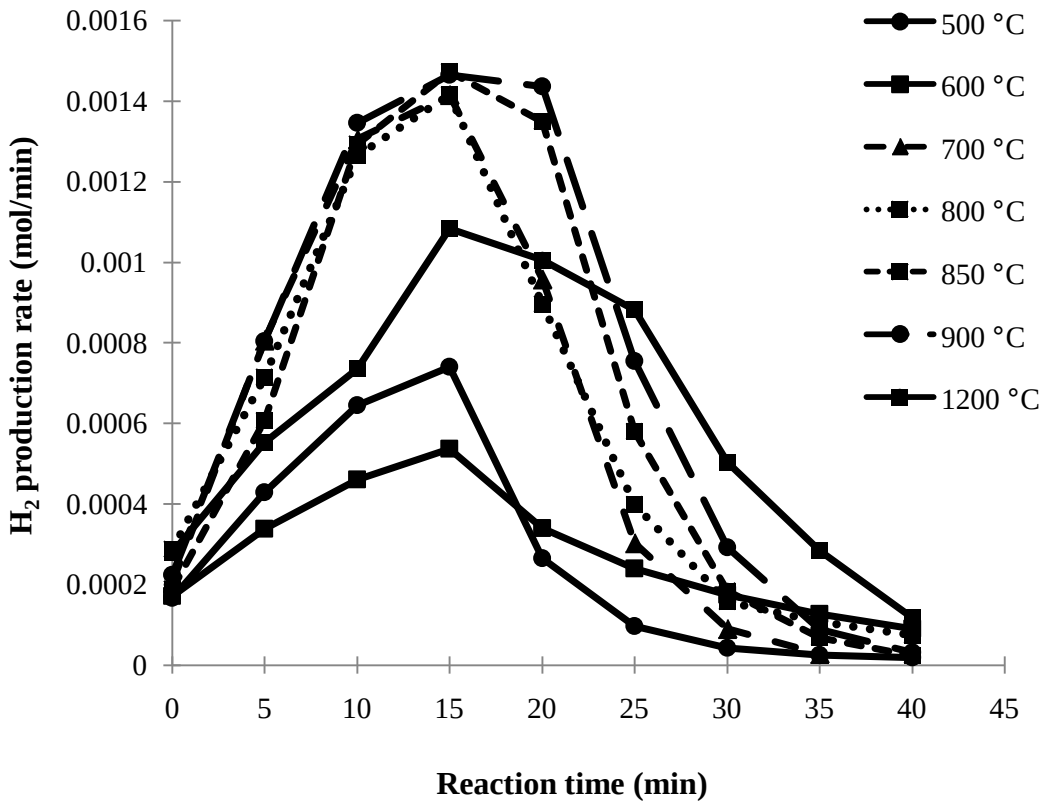


**Figure 4.14** Rate of $H_2$ production respect to with time, from the reaction temperature in the range of 500 to 1200 $^oC$. Zinc evaporation temperature was fixed at 850 $^oC$, while the flow rate nitrogen gas, zinc vapor and supplied steam were 1, 1.5 and 0.5 l/min, respectively.

In experiments in this section Zn foil was evaporated to become Zn vapor at temperature of 850 $^{o}$C. Therefore, competition between hydrolysis of Zn vapor with steam in homogeneous phase and condensation of Zn vapor to Zn particles and subsequent hydrolysis of Zn particles with steam in heterogynous phase took place. If the reaction temperature was higher than evaporation temperature, it would result in no condensation of Zn vapor to Zn particles. Then the hydrolysis of Zn took place only in homogeneous phase. From the Figure 4.15 shows yield of $H_2$ gas produced and fraction of ZnO in the product collected in the filter, when the reaction temperature was varied from 500 to 1200 $^{o}$C. It was found that when the reaction temperature was increased from 500 to 900 $^{o}$C, the yield of $H_2$ increased from 24.4 % to 59.71%. As the reaction temperature was increased, fraction of Zn vapor condensing to Zn particles was lowered. According to other researches, it was found that the $H_2$ gas formation by hydrolysis of Zn vapor with steam in homogeneous phase was favored over the heterogeneous phase reaction [11, 13]. Moreover, according to the Arrhenius Equation, the increased temperature results in increased reaction rate constant (k). However, at the reaction temperatures of 1200 $^{o}$C, yield of $H_2$ decreased from the value observed at 900 $^{o}$C, because reaction temperature of 1200 $^{o}$C was too high and hydrolysis of zinc vapor with steam was exothermic reaction. Moreover, when increasing the reaction temperature, resulted in fraction of ZnO in the product slightly increasing. It can be explained that high reaction temperature resulted in, reaction will be better occurred and mole fraction of ZnO increased from 16.9 to 30.17 %.

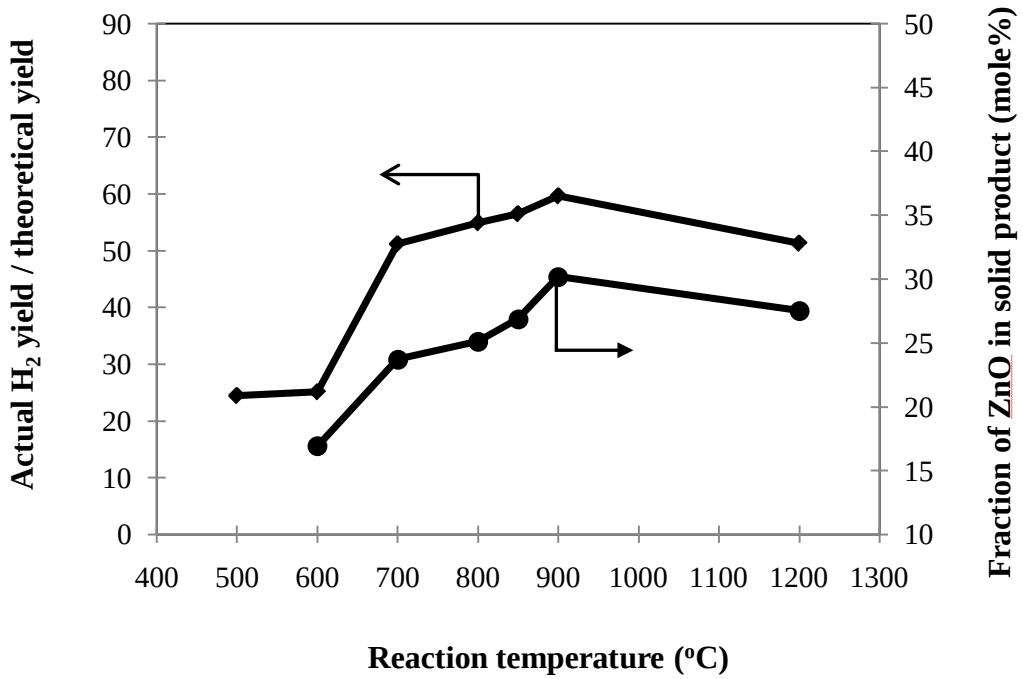


**Figure 4.15** Actual $H_2$ yield / theoretical yield and fraction of ZnO (mole %) in the product collected by the filter as function of reaction temperature.

Figure 4.16 shows SEM micrographs of products collected by the filter. It was found that when the reaction temperature was increased from 500 to 600 $^{o}$C, the particle size was increased. It was suggested that the reaction temperature of 500 and 600 $^{o}$C was low temperature, such that Zn vapor could condense into Zn particles and subsequently resulted in the heterogeneous hydrolysis of Zn vapor with steam. Supplied steam reacted at surface of zinc particle and form to ZnO layer covering zinc particle. These findings were further supported by TEM pictures [16]. When the reaction temperature was increased from 700 to 900 $^{o}$C, sizes of the particles were increased. In this resulted, when increasing the reaction temperature due to the increasing reaction rate, as shown in Figure 4.16(c) to 4.16(f). Average diameters of the particulate product were measured by an image processing program (SemAfore 4.0), based on 50 randomly selected particles from SEM images. It was found that when the reaction temperature was increased, the average diameter of the particulate product was increased. The average diameters of the particulate product were 312, 325, 329 and 344 nm where the reaction temperature as 700, 800, 850 and 900 $^{o}$C, respectively.

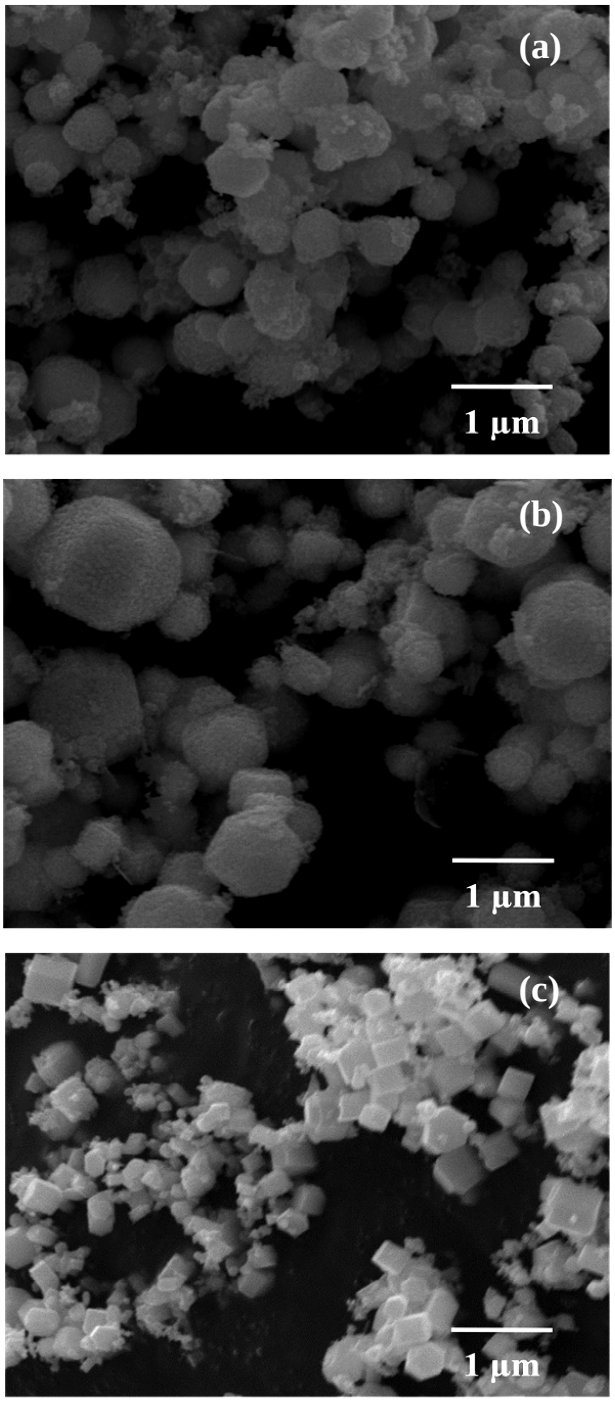


**Figure 4.16** SEM micrographs of products collected by filter when the reaction temperature was set at 500 (a), 600 (b), 700 (c), 800 (d), 850 (e), and 900 $^{o}$C (f).

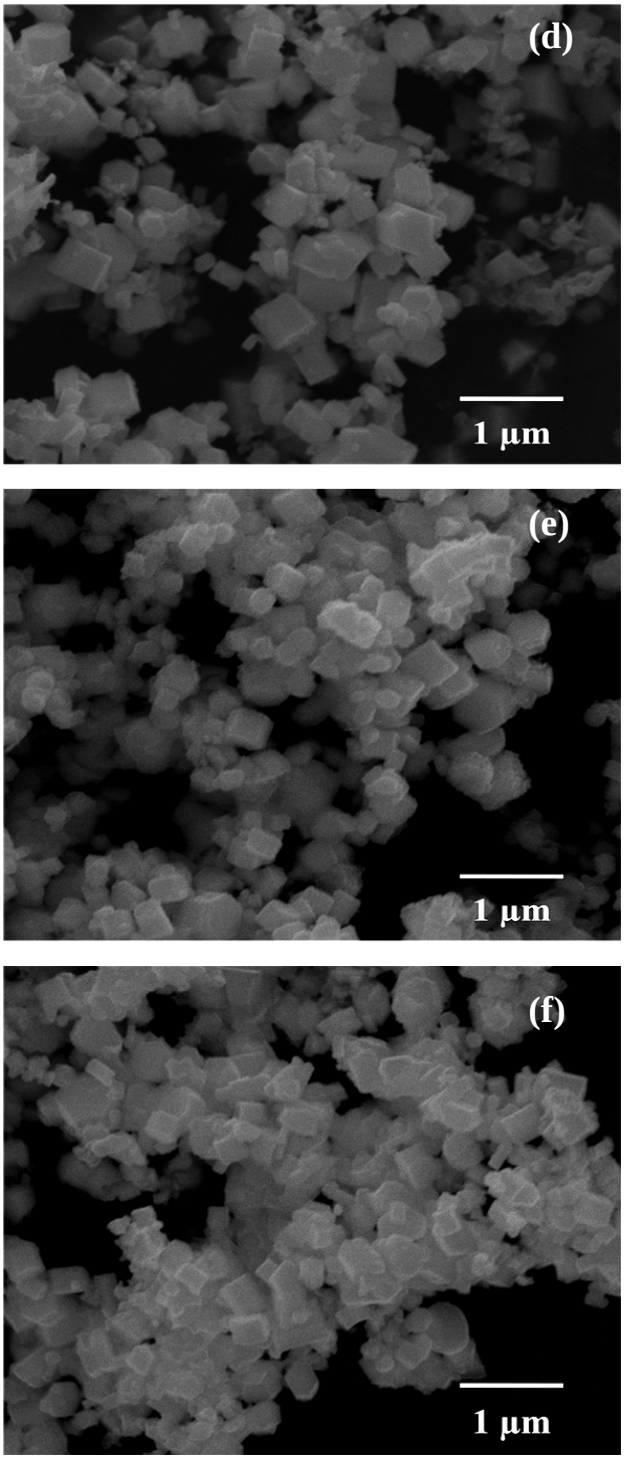


Figure 4.16 (continued)

The amounts of product deposited at different positions of the system are shown in Table 4.3. It can be seen that the amount of product collected at the reaction zone, outlet zone and collecting system increased with increasing reaction temperature. Because the hydrolysis reaction at higher temperature was more aggressive, and consequently the more ZnO product was formed and deposited in all parts of the reactor.

Table 4.3 The amount of the products collected at each position of the system from the reaction at temperature.

| **Reaction temperature (˚C)** | **Amount of solid product collected** | | | | |
|---|---|---|---|---|---|
| | **Reaction zone (g)** | **Outlet zone (g)** | **Collecting system (g)** | **Filter (g)** | **Total (g)** |
| 500 | 0.212 | 0.043 | 1.106 | 1.747 | 3.106 |
| 600 | 0.244 | 0.047 | 1.132 | 1.572 | 2.995 |
| 700 | 0.321 | 0.086 | 1.147 | 1.524 | 3.078 |
| 800 | 0.360 | 0.103 | 1.295 | 1.217 | 2.975 |
| 850 | 0.364 | 0.110 | 1.306 | 1.323 | 3.103 |
| 900 | 0.371 | 0.147 | 1.345 | 1.135 | 2.998 |

From results reported earlier, it was found that low Zn vapor flow rate and high reaction temperature resulted in increasing yield of $H_2$ gas. Since this research tried to find optimal condition to produce $H_2$ gas, it was chosen to further investigate effect of Zn vapor flow rate at reaction temperature of 900 $^oC$. The results are shown in Figure 4.17.

From Figure 4.17 it was found that as the flow rate of the carrier gas for zinc vapor was increased, the reaction time, when the highest of $H_2$ production rate was reached, was decreased. This can be explained that as the flow rate of the carrier gas for zinc vapor was increased, the rate of evaporation of zinc foil was also increased. Moreover, since the amount of zinc foil put in to the reactor was the same for all experiments. That is why $H_2$ production diminished faster when the Ar flow rate of 1.5 l/min was used.

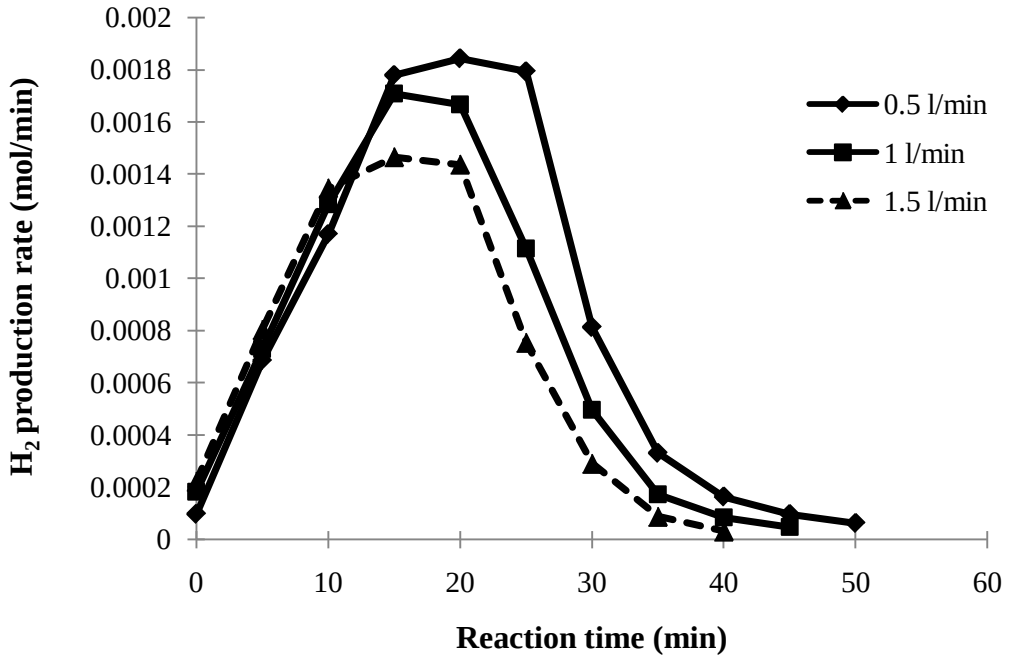


**Figure 4.17** Rate of $H_2$ production with respect to reaction time, using flow rate of the carrier gas (Ar) for zinc vapor of 0.5, 1 and 1.5 l/min. For this set of experiment, the zinc evaporation temperature was fixed at 850 $^oC$. The reaction temperature was fixed at 900 $^oC$. Flow rate of nitrogen gas and supplied steam was kept at 1 and 0.5 l/min, respectively.

From Figure 4.18, it was found that yield of $H_2$ gas was decreased when Zn vapor flow rate was increased. Moreover, increasing Zn vapor flow rate resulted in increasing fraction of ZnO in the collected product. The residence time should be the factor influencing this result as previously discussed. Increasing the zinc vapor flow rate from 0.5 l/min to 1.5 l/min resulted in the increase in yield of $H_2$ gas from 59.71 to 72.59 % and the increase in mole fraction of ZnO from 21.83 to 29.40 %. Moreover, by comparing the results from the experiments using the same flow rate, yield of $H_2$ gas and fraction of ZnO at the reaction temperature of 900 $^oC$ were higher than these obtained at temperature of 700 $^oC$ as shown in Figure 4.19.

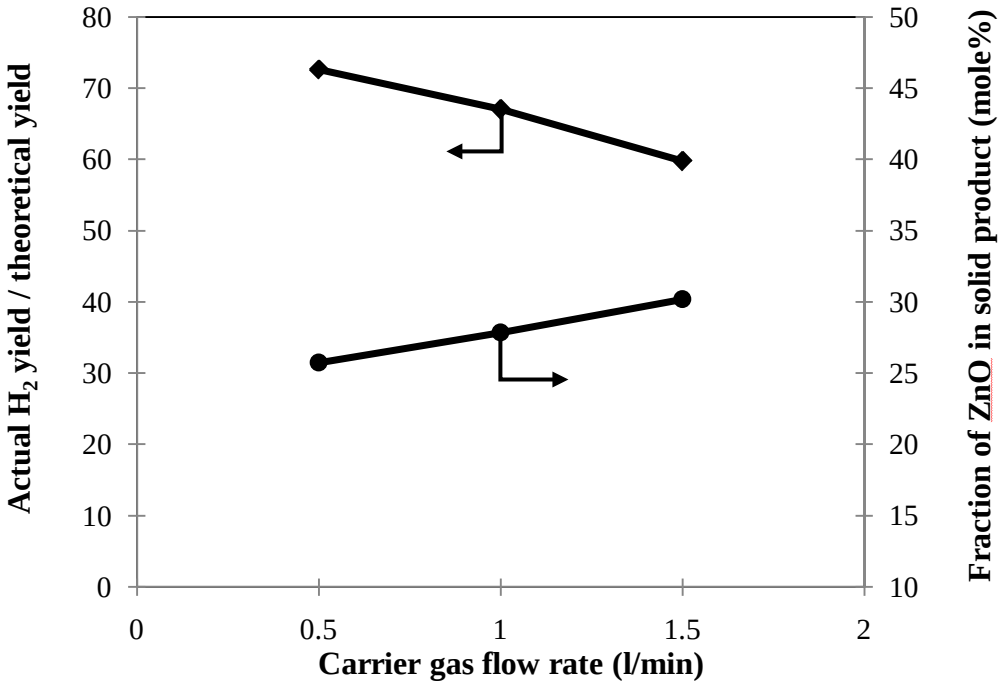


**Figure 4.18** Actual $H_2$ yield / theoretical yield and fraction of ZnO (mole %) in the product collected by the filter as function of carrier gas flow rate.

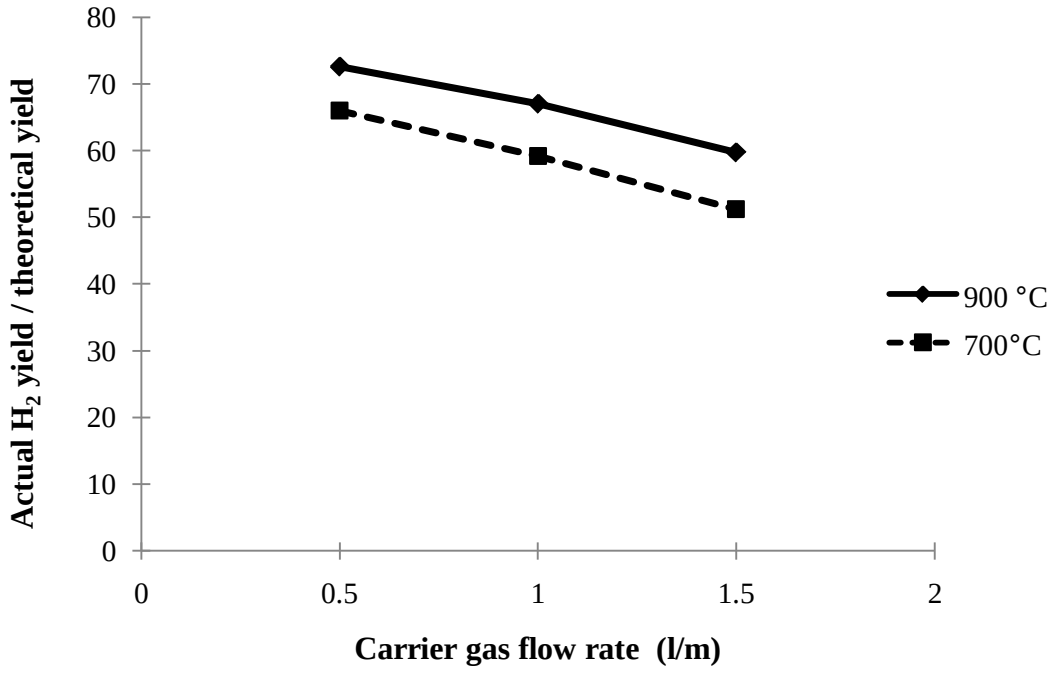


**Figure 4.19** Actual yield of $H_2$ gas as function of Zn vapor flow rate at reaction temperature 700 $^{o}$C and 900 $^{o}$C.

### 4.4 Effect of Resident Time

The effect of resident time was studied by varying length the reaction zone (i.e., the distance from inlet tube to outlet tube) at 1, 2, 3 and 4 cm respectively. The evaporation temperature was fixed at 850 $^{o}$C, while the reaction temperature was fixed at 900 $^{o}$C. Flow rats of nitrogen gas, zinc vapor and supplied steam were kept at 1, 0.5 and 0.5 l/min, respectively.

In this section, experimental-setup is shown in Figure 4.19. For all experiments, the position of inlet alumina tubes and the position of zinc foil were fixed, but the position of the outlet alumina tube was varied by moving toward the inlet tubes.

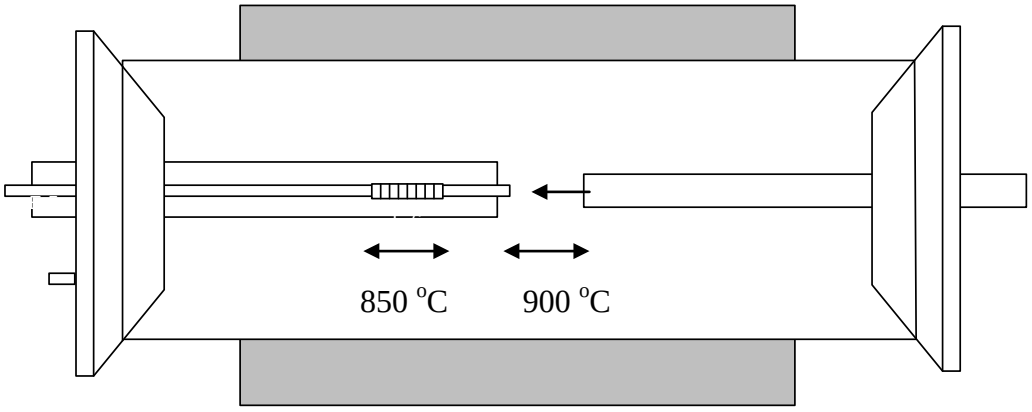


**Figure 4.20** Experimental-setup for the studies of the effect of resident time.

Figure 4.21 shows rate of $H_2$ gas production with respect to reaction time. It was found that as the length of the reaction zone was increased, it resulted in increasing rate of $H_2$ gas production. Moreover, the highest rate of $H_2$ gas production was reached at the reaction time of 20 min, while the $H_2$ production ceased after the reaction time of 50 min for all experiments. It can be explained by as the flow rate of the carrier gas for zinc vapor was constant, the rate of evaporation of zinc foil was also constant. Moreover, the amount of zinc foil put in to the reactor was the same for all experiments. That is why $H_2$ production ceased after the reaction time of 50 min.

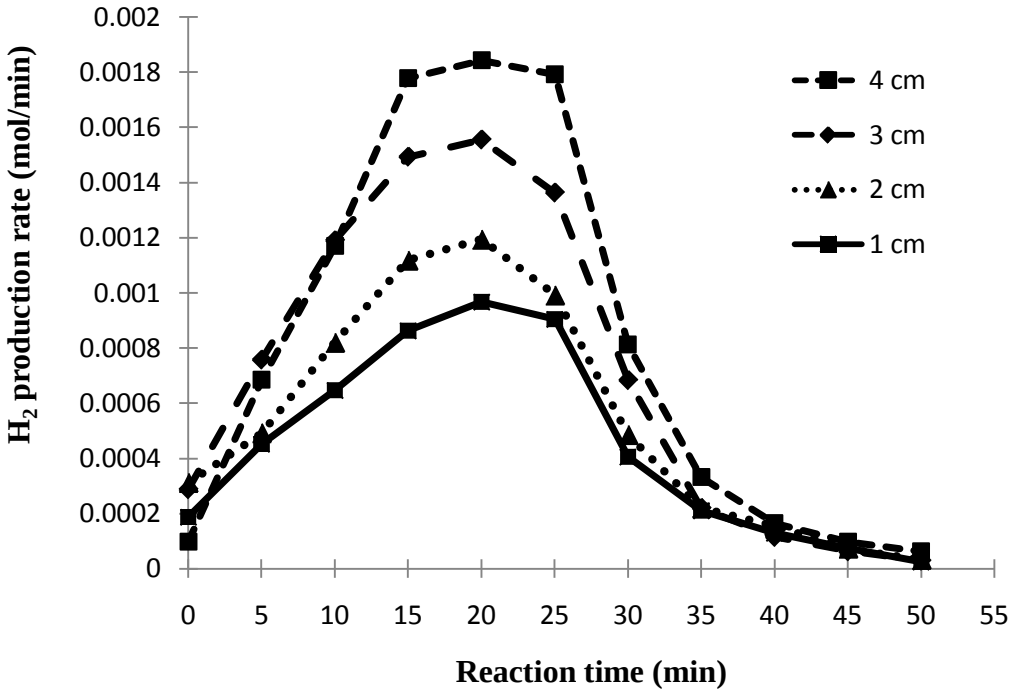


**Figure 4.21** Rate of $H_2$ production with respect to reaction time, using length of reaction zone 1, 2, 3 and 4 cm. For this set of experiment, the zinc evaporation temperature was fixed at 850 $^{o}$C. The reaction temperature was fixed at 900 $^{o}$C. Flow rate of nitrogen gas, supplied steam and Zn vapor was kept at 1, 0.5 and 0.5 l/min, respectively.

Figure 4.22 shows yield of $H_2$ as a function of the length of reaction zone. It can be seen that when the length of the reaction zone was decreased, the yield of $H_2$ gas was decreased. It can be explained that the short reaction zone provided shot residence time for the reaction. This means that zinc and steam had less time to react. Therefore, yield of $H_2$ gas was decreased. The highest of $H_2$ yield was 72.59 % when reaction zone distant was 4 cm. Moreover, fraction of ZnO in the product collected by the filter was increased when reaction zone was shorten. This is because the shorter distance increases a chance for the product to come straight through the outlet tube to the collecting system. The highest mole fraction of ZnO in the product collected by the filter was 33.2 % when reaction zone distant was 4 cm.

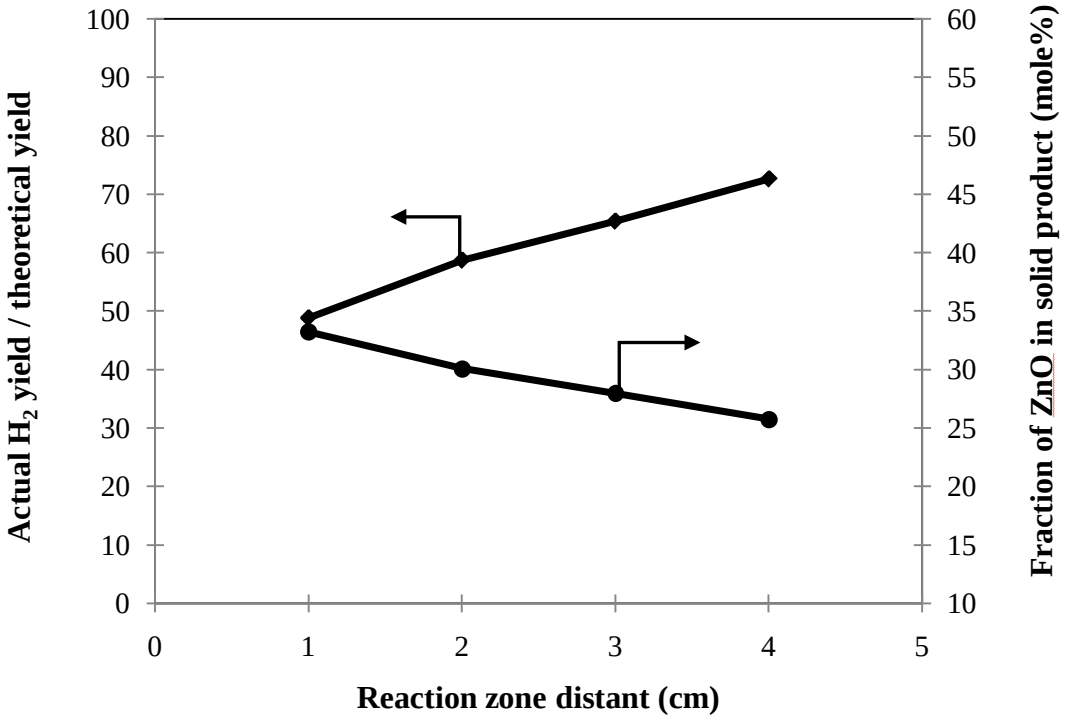


**Figure 4.22** Actual $H_2$ yield / theoretical yield and fraction of ZnO (mole %) in the product collected by the filter as function of reaction distance. For this set of experiment, the zinc evaporation temperature was fixed at 850 $^{o}$C. The reaction temperature was fixed at 900 $^{o}$C. Flow rate of nitrogen gas, supplied steam and Zn vapor was kept at 1, 0.5 and 0.5 l/min, respectively.

Observing from the SEM image in Figure 4.23a, it was found that shot reaction zone resulted in particles with smaller size with less degree of agglomeration. While the increasing in length of the reaction zone, caused the particles to be larger size with higher degree of agglomeration, as shown in Figure 4.22b. This is because the longer distance offers the longer time for the reaction to occur and consequently the products grew larger into the collecting system.

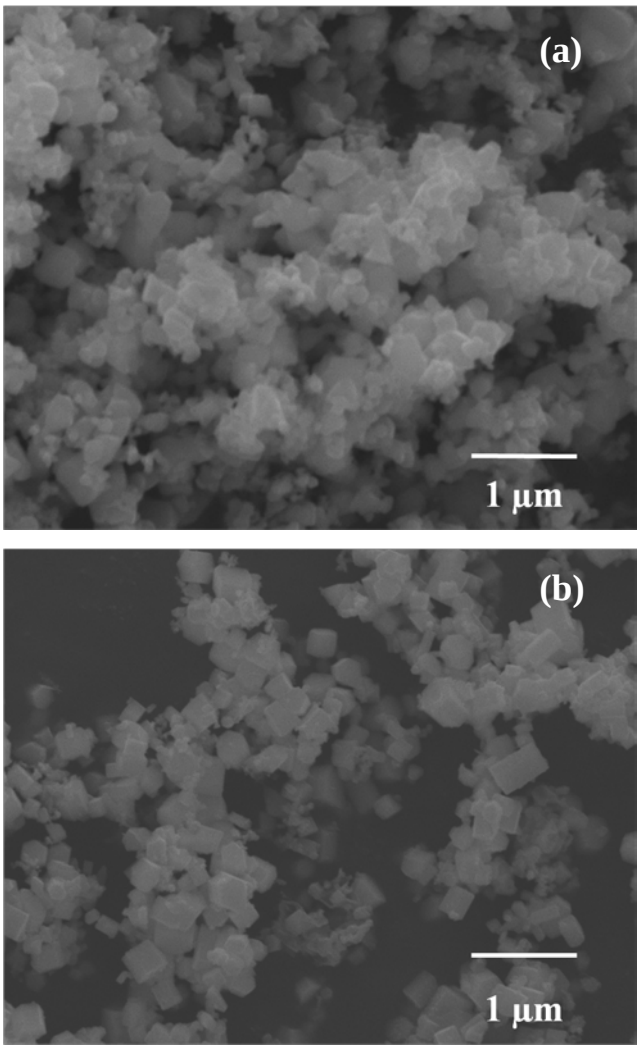


**Figure 4.23** SEM micrographs of products collected by filter when reaction zone distance was increased from 1 cm (a) and 4 cm (b).

The amounts of product obtained from the reaction using different length of the reaction zone, are shown in Table 4.4. It can be seen from the table that the short reaction zone caused the low particles to deposit in the reaction zone. While the long reaction zone, resulted in the high particles to deposit in the reaction zone.

**Table 4.4** The amount of the products collected at each position of the system from the reaction with different length of reaction zone.

| Distance of reaction zone (cm) | Amount of solid product collected | | | | |
|---|---|---|---|---|---|
| | Reaction zone (g) | Outlet zone (g) | Collecting system (g) | Filter (g) | Total (g) |
| 1 | 0.274 | 0.073 | 1.288 | 1.330 | 2.965 |
| 2 | 0.489 | 0.092 | 1.257 | 1.175 | 3.013 |
| 3 | 0.651 | 0.107 | 1.186 | 1.151 | 3.095 |
| 4 | 0.735 | 0.118 | 1.154 | 1.061 | 3.068 |

### 4.5 Distribution of ZnO depositited in the system

This section, to investigate fraction of ZnO in the product was deposited in the reaction zone, outlet zone, chamber and the filter. Flow rate of the carrier gas (Ar) for zinc vapor was 0.5 l/min. The zinc evaporation temperature was fixed at 850 $^{o}$C. The reaction temperature was fixed at 900 $^{o}$C. Flow rate of nitrogen gas and supplied steam was kept at 1 and 0.5 l/min, respectively.

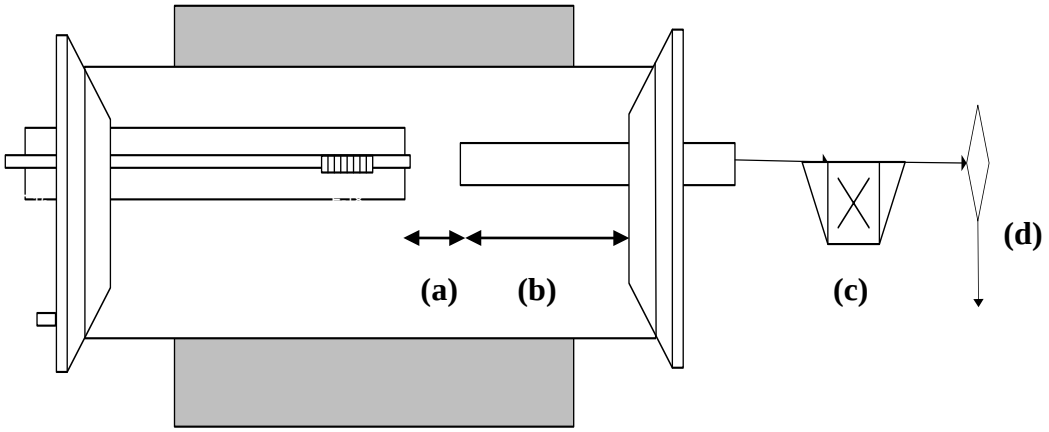


**Figure 4.24** Experimental-setup for the studies of the effect of deposition of ZnO in the system; reaction zone (a), collecting tube (b), chamber (c) and filter (d).

Fractions of ZnO in the products deposited at different position of the system are shown in the Figure 4.25. It was found that mole fractions of ZnO in the reaction zone, in the collecting tube, in the collecting chamber and in the filter were 100, 89.02, 53.89 and 25.82 mole %, respectively. It can be explained that since temperature at the reaction zone in this experiment was above the evaporation temperature of zinc, condensation of Zn vapor did not take place. Therefore, the formation of ZnO by hydrolysis of Zn vapor took place homogeneously in gas phase in agreement with Weidenkaff et al. [16]. However, the temperature in the collecting tube was lower than the evaporation temperature of zinc, such that Zn vapor could condense in to Zn particles. So fraction of ZnO deposited in the reaction zone was higher than in the collecting tube. Moreover, fraction of ZnO deposited in the collecting chamber was higher than that in the filter because particles of ZnO product were larger size than Zn particles. When the particles of the product passed through the chamber, more ZnO particles deposited in the chamber than Zn particles. Moreover, this condition resulted in yield of $H_2$ at 72.59 % relative to the theoretical $H_2$ yield, but the yield of ZnO (calculated from ICP) was only 49.2 %. The theoretical yield of $H_2$ should be equal yield of ZnO product, but in this result, the yield of ZnO product was lower than the yield of $H_2$ gas because the loss of particles product in the equipment of the system. According to the calculation, it was found that Zn loss was 16.019 %. It could be observed by the calculation of Zn balance, as shown in Appendix F. Moreover, according to other researches, the supplied steam could not decomposed to form $H_2$ gas at this temperature. The supplied steam could be decomposed only when temperature was higher than 1500 $^oC$ [17].

In this section, to found Zn foil loss when heat up temperature. The flow rate of $N_2$ gas was 1 l/min, initial Zn foil was 3.2 g and ramp rate of reactor was 10 $^oC$/min. The evaporation temperature was 850 l/min. It was found that Zn loss 0.03 g

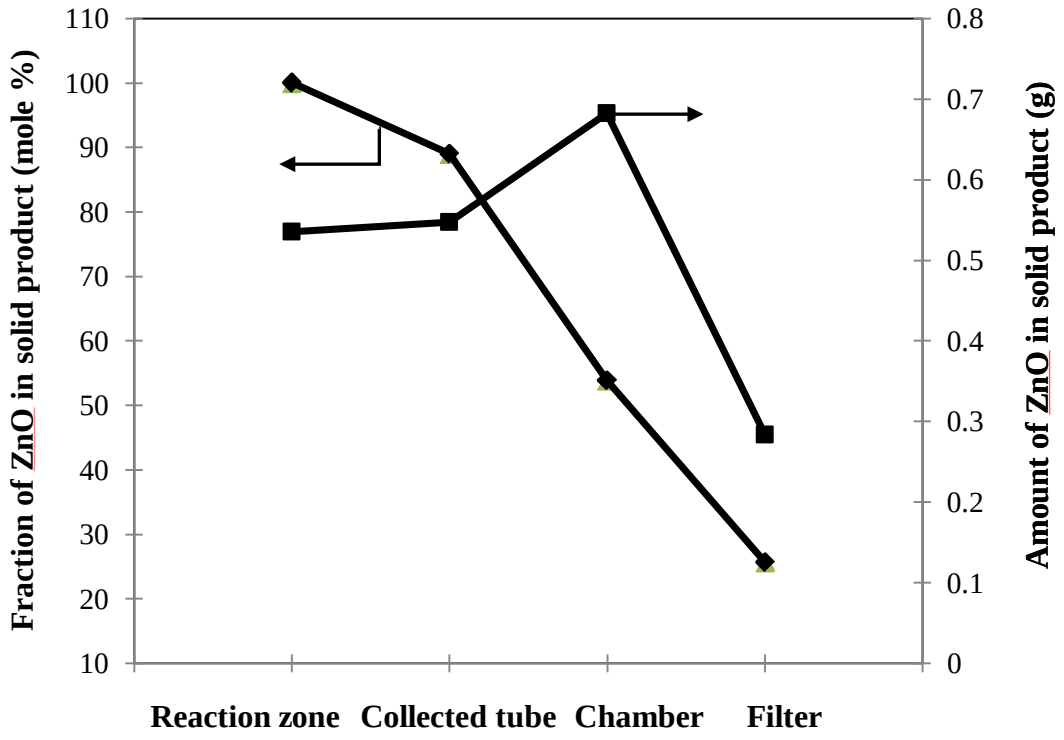


**Figure 4.25** Fraction of ZnO and amount of ZnO in the product deposited in the reaction zone, collected tube, collecting system and filter.

## 4.6 Transport phenomena in the system

### 4.5.1 At Zn evaporation Zone

Maximum vaporization of Zn foil could be achieved when partial pressure of Zn vapor is equal to vapor pressure of Zn. With increasing evaporation temperature, the vapor pressure of Zn is increased. So more Zn foil is vaporized when the evaporation temperature is increased. Furthermore, at the fixed evaporation temperature, the increased flow rate of the carrier gas results in faster vaporization of Zn foil. It is suggested that the vaporization of zinc in this work is induced mass transfer limited.

### 4.5.2 At reaction Zone

In this research, the hydrolysis of Zn with supplied steam occurred homogeneously as Zn vapor reacted with steam, and heterogeneously as Zn particles reacted with steam.

In this research, Zn vapor and steam were supplied parallel flow in to the reaction zone. The reaction occurred when Zn vapor and steam diffused towered each other in radial direction. For the homogeneous reaction, when the concentration of Zn vapor was increased, it resulted in increasing mass transfer between Zn vapor and steam. The reaction rate became higher as well. For the heterogeneous reaction, steam reacted at surface of Zn particles to form ZnO layer covering Zn particles. Therefore, rate of hydrolysis reaction was limited by the diffusion of Zn through ZnO layer [18].

Although hydrolysis reaction is exothermic, rate of the hydrolysis reaction is slow as witnessed from the fact that majority of the collected solid were still zinc. Therefore, the reaction temperature increased only slightly so that heat transfer did not affect in the reaction.

# CHAPTER V

## CONCLUSIONS AND RECOMMENDATIONS

### 5.1 Conclusions

In this work the synthesis of zinc oxide nanoparticles and $H_2$ production by Hydrolysis of zinc vapor process and use zinc foil as source material. The aim of this research is to find optimal condition for synthesis ZnO nanaparticle and $H_2$ gas product. The effects of evaporation temperature, flow rate of carrier gas for zinc vapor, reaction temperature and resident time were investigated.

According to above mentioned experimental results, it can be concluded as follows.

1. Evaporation temperature effect on concentration of Zn vapor, when increasing evaporation temperature resulted in higher yield of $H_2$ gas product and the larger size of particle.

2. Flow rate of carrier gas for zinc vapor effects on resident time and concentration of zinc vapor. It was suggested that when carrier gas flow rates was increased yield of $H_2$ gas product was decreasing. Moreover, higher carrier gas flow rate resulted in higher particles size.

3. When reaction temperature was increased resulting in yield of $H_2$ gas product was increased.

4. The distance of reaction zone had to effect on resident time for the reaction. It was found that short reaction zone provide short resident time for the reaction. Therefore yield of $H_2$ gas was decreased and particles size was increased.

## 5.2 Recommendations for future work

According to the experimental results in this work, yield of $H_2$ gas is calculated from GC and frequency of the record data had to result for yield $H_2$ gas product. It should be verified these results by more frequency in collected data or used GC online. Moreover, yield of ZnO should be observed in all experiment.

## References


[1] K. Wegner and S. E. Pratsinis, Scale-up of nanoparticle synthesis in diffusion flame reactors, Chemical Engineering Science 58 (2003): 4581-4589.

[2] Z. L. Wang, Zinc oxide nanostructures: Growth, properties and applications, Journal of Physics Condensed Matter 16 (2004).

[3] S. J. Chen, G. R. Wang, and Y. C. Liu, The structure and photoluminescence properties of ZnO nanobelts prepared by a thermal evaporation process, Journal of Luminescence,129 (2009): 340-343.

[4] M. Rosina, P. Ferret, P. H. Jouneau, I. C. Robin, F. Levy, G. Feuillet, and M. Lafossas, Morphology and growth mechanism of aligned ZnO nanorods grown by catalyst-free MOCVD, Microelectronics Journal 40 (2009): 242-245.

[5] X. Zong and P. Wang, Effect of UV irradiation on the properties of ZnO nanorod arrays prepared by hydrothermal method, Physica E: Low Dimensional Systems and Nanostructures 41 (2009): 757-761.

[6] R. J. Weiss, H. C. Ly, K. Wegner, S. E. Pratsinis, and A. Steinfeld, $H_2$ production by Zn hydrolysis in a hot-wall aerosol reactor, AIChE Journal 51 (2005): 1966-1970.

[7] A. Steinfeld, Solar thermochemical production of hydrogen - A review, Solar Energy 78 (2005): 603-615.

[8] J. A. Clarke and D. J. Fray, Oxydation of Zinc vapor by hydyogen- water vapour mixtures, Transactions of the Institution of Mining and Metallurgy, Section C: Mineral Processing and Extractive Metallurgy 88 (1979).

[9] A. Nirmolo, H. Woche, and E. Specht, Mixing of jets in cross flow after double rows of radial injections, Chemical Engineering and Technology 31 (2008): 294-300.

[10] K. Wegner, H. C. Ly, R. J. Weiss, S. E. Pratsinis, and A. Steinfeld, In situ formation and hydrolysis of Zn nanoparticles for $H_2$ production by the 2-step ZnO/Zn water-splitting thermochemical cycle, International Journal of Hydrogen Energy 31(2006): 55-61.

[11] F. O. Ernst, A. Tricoli, S. E. Pratsinis, and A. Steinfeld, Co-synthesis of $H_2$ and ZnO by in-situ Zn aerosol formation and hydrolysis, AIChE Journal 52 (2006): 3297-3303.

[12] T. Melchior, N. Piatkowski, and A. Steinfeld, $H_2$ production by steam-quenching of Zn vapor in a hot-wall aerosol flow reactor, Chemical Engineering Science 64 (2009): 1095-1101.

[13] H. H. Funke, H. Diaz, X. Liang, C. S. Carney, A. W. Weimer, and P. Li, Hydrogen generation by hydrolysis of zinc powder aerosol, International Journal of Hydrogen Energy 33 (2008): 1127-1134.

[14] F. O. Ernst, A. Steinfeld, and S. E. Pratsinis, Hydrolysis rate of submicron Zn particles for solar $H_2$ synthesis, International Journal of Hydrogen Energy 34 (2009): 1166-1175.

[15] X. Ma and M. R. Zachariah, Size-resolved kinetics of Zn nanocrystal hydrolysis for hydrogen generation, International Journal of Hydrogen Energy 35 (2010): 2268-2277.

[16] R. Weiss H. Ly, K. Wegner, S. Pratsinis, and A. Steinfeld, $H_2$ production by Zn hydrolysis in a hot-wall aerosol reactor, AIChE Journal, inpress.

[17] T. Nakamura, Hydrogen production from water utilizing solar heat at high temperatures, Solar Energy 35 (1977): 467-475.

# APPENDICES

# APPENDIX A

# CALCULATION OF REACTANT FLOW RATE

## Vapor pressure of steam

The vapour pressure of water is the pressure at which steam is saturated. At higher pressures water would condense. Vapour pressure is a function of temperature.

## Antoine equation

$$\log_{10} P = A - \frac{B}{C + T}$$

Where the temperature T is in degrees Celsius and the vapor pressure P is in mmHg. The constants are given as

| | *A* | *B* | *C* | *T* min. °C | *T* max °C |
|---|---|---|---|---|---|
| Water | 8.07131 | 1730.63 | 233.426 | 1 | 100 |
| Water | 8.14019 | 1810.94 | 244.485 | 99 | 374 |

http://en.wikipedia.org/wiki/Vapour_pressure_of_water

$$\log P = 8.07131 - \frac{1730.63}{233.426+95}$$

$\log P = 2.8018$

$P = 633.577$ mmHg

$P = 0.834$ atm

We assume that pressure in Steam trap is 1 atm.

$$x_A = n_A/n$$

$$p_A = x_A * p$$

where : n = total moles of the gas mixture

$p_A$ = partial pressure of gas component A in gas mixture

$n_A$ = moles of gas component A in gas mixture

$x_A$ = moles fraction of gas component A in gas mixture

p = pressure of gas mixture

$x_{water} = 0.834/1$

$x_{water} = 0.834$

For example, in case of Ar carrier for steam flow rate 0.5 L/min and zinc vapor flow rate 1.5 L/min. Zn raw material 3.2 g was exhausted in time 35 min under evaporation temperature 750 $^oC$

$$\text{Rate of Zn generation} = \frac{3.2\ [g]}{35[min] \times 65.38\ [g/mole]}$$

$$= 1.398 \times 10^{-3}\ \text{mole/min}$$

$$\text{Rate of steam} = \frac{0.5\ [L/min] \times 0.834 \times 1.783\ [g/L]}{39.948[g/mole]}$$

$$= 1.861 \times 10^{-2}\ \text{mole/min}$$

# APPENDIX B

## TEMPERATURE PROFILE INSIDE REACTOR

Temperature profile inside the reactor was mapped, as shown in Figure B1. We found that the temperature inside the reactor slightly decrease in the desired temperature from 28 to 32 cm. Base on this data, the effective zone for evaporation was taken be 28 to 32 cm of the furnace, from the feed-side of the reactor.

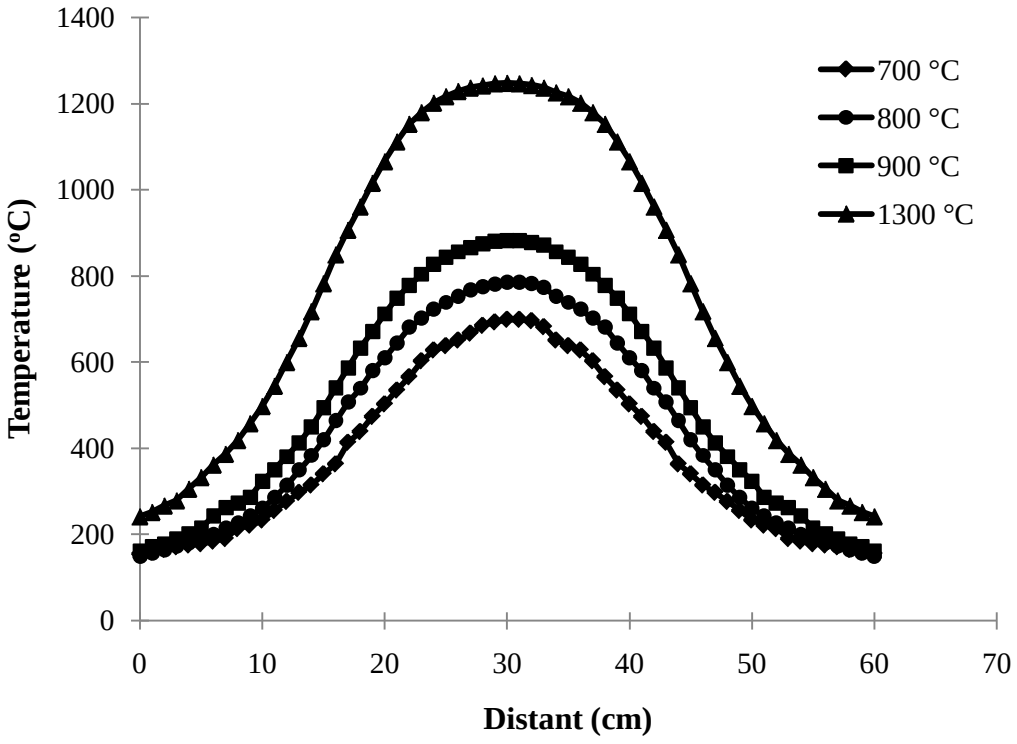


**Figure B1** Temperature profiles inside the reactor.

# APPENDIX C

## CALIBRATION OF GAS CHROMATOGRAPHY

Condition of Gas chromatography

TCD GC8A
colume Molecular sieve
carrier gas Ar
flow carrier gas 40 ml/min
Temp $^{o}$C
Injector 100
column 70
detector 70

Mole of $H_2$ gas product can be calculated from n=PV/RT

P = 1 atm
R = 82.06 $cm_3$.atm/(mol.K)
T = 303 K

| volume(cm3) | mole$H_2$(mol) | Retention time (s) | | | | Area | | | |
|---|---|---|---|---|---|---|---|---|---|
| | | 1 | 2 | 3 | Average | 1 | 2 | 3 | Average |
| 0 | 0 | 0 | 0 | 0 | 0 | 0 | 0 | 0 | 0 |
| 0.05 | 2.01092E-06 | 1.327 | 1.323 | 1.322 | 1.324 | 333631 | 333908 | 332557 | 333365.33 |
| 0.1 | 4.02185E-06 | 1.343 | 1.347 | 1.347 | 1.34566667 | 891847 | 913237 | 930953 | 912012.33 |
| 0.15 | 6.03277E-06 | 1.362 | 1.362 | 1.354 | 1.35933333 | 1410698 | 1345355 | 1349837 | 1368630 |
| 0.2 | 8.0437E-06 | 1.368 | 1.37 | 1.371 | 1.36966667 | 1824215 | 1797598 | 1824130 | 1815314.3 |
| 0.25 | 1.00546E-05 | 1.381 | 1.384 | 1.376 | 1.38033333 | 2208988 | 2281590 | 2069219 | 2186599 |

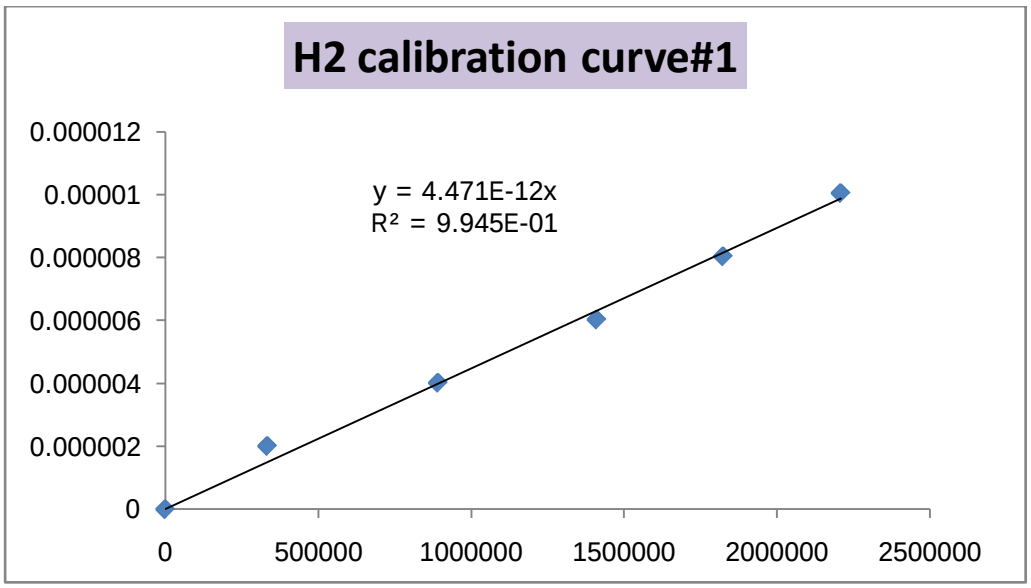


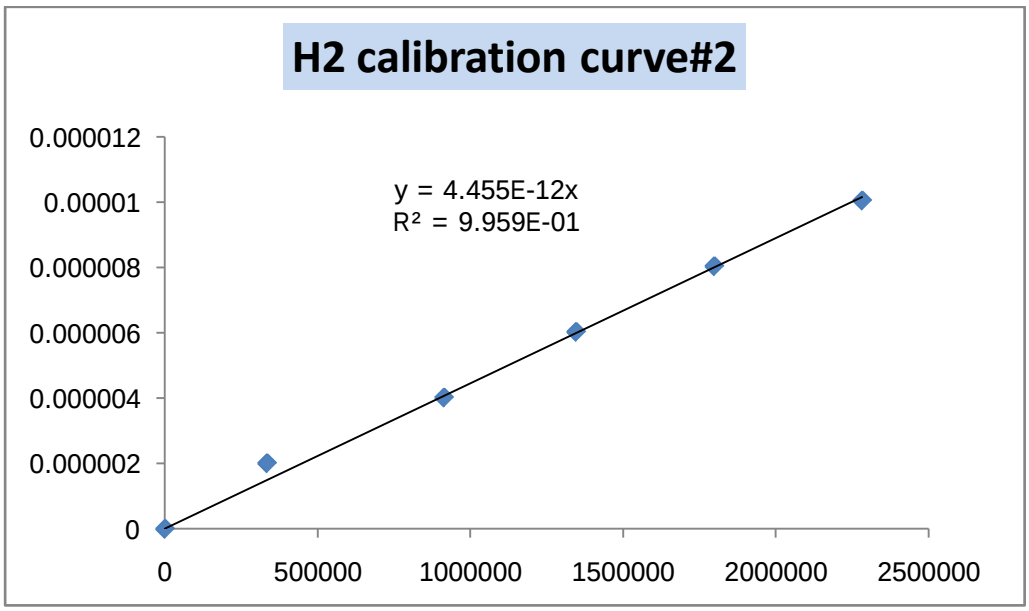


**Figure C1** H2 calibration curve; mole $H_2$ gas (axial y), volume of gas were injected to GC (axial x)

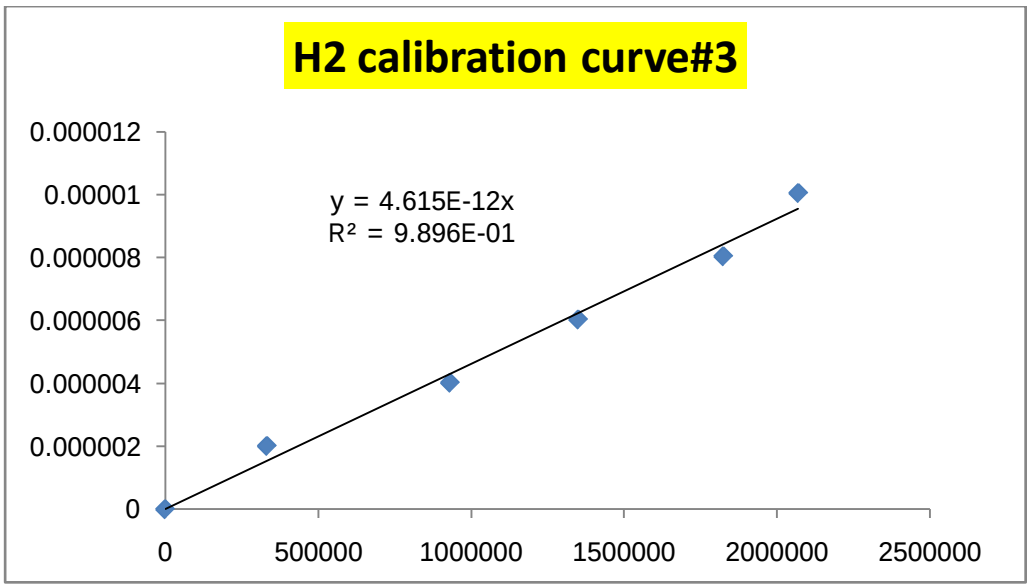


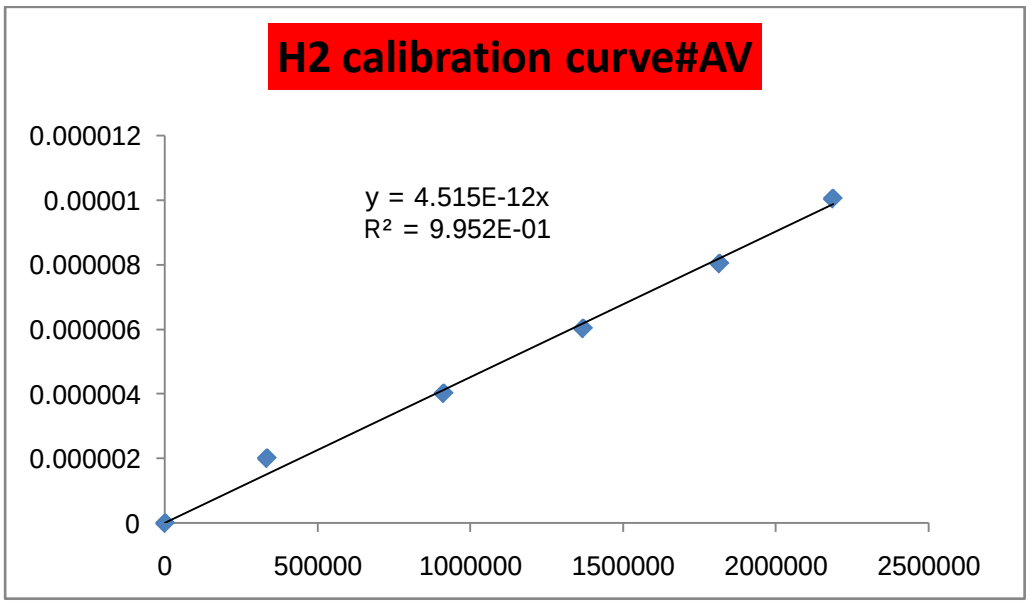


Figure C1 continued

# APPENDIX D

## CALCULATION %YIELD OF HYDROGEN GAS PRODUCT

Yield of $H_2$ (%) gas product can be calculated from $H_2$ calibration curve

$$y = 4.515E\text{-}12x$$

y = mole of $H_2$ / volume of gas inject (mol/$cm^3$)

x = area from GC ($cm^2$)

Mole of $H_2$ (mol/min) = y (mol/$cm^3$) x Total gas flow rate ($cm^3$/min)

Plot graph between Mole of $H_2$ (mol/min) and reaction time (min) and find area under graph from OriginPro 7.5 Program. Area under graph is mole total of $H_2$ gas product

For example, in case of Ar carrier for steam flow rate 0.5 L/min and zinc vapor flow rate 0.5 L/min and $N_2$ gas flow rate 1 L/min. Zn raw material 3.369 g was exhausted in time 45 min under evaporation temperature 850 $^oC$ and reaction temperature 700 $^oC$

| mole/1ml | flow rate(ml/min) | slope | area | Time(min) | mole/min |
|---|---|---|---|---|---|
| 8.87E-08 | 2000 | 4.515E-12 | 19649 | 0 | 0.000177 |
| 2.72E-07 | 2000 | 4.515E-12 | 60280 | 5 | 0.000544 |
| 4.96E-07 | 2000 | 4.515E-12 | 109933 | 10 | 0.000993 |
| 7.25E-07 | 2000 | 4.515E-12 | 160533 | 15 | 0.00145 |
| 9.19E-07 | 2000 | 4.515E-12 | 203528 | 20 | 0.001838 |
| 7.39E-07 | 2000 | 4.515E-12 | 163655 | 25 | 0.001478 |
| 3.09E-07 | 2000 | 4.515E-12 | 68367 | 30 | 0.000617 |
| 9.3E-08 | 2000 | 4.515E-12 | 20606 | 35 | 0.000186 |
| 3.17E-08 | 2000 | 4.515E-12 | 7021 | 40 | 6.34E-05 |
| 1.07E-08 | 2000 | 4.515E-12 | 2360 | 45 | 2.13E-05 |

Total area from integration of under the graph = 0.03634 mole

Total mole of $H_2$ gas product from reaction = 0.03634 mole

Total mole of $H_2$ gas product from theoretical

Zn foil initial = 3.369 g

Zn foil final = 0 g

Zn was evaporated = 3.369 g

Zn was evaporated = 0.0413841 mole

$H_2$ from theorem = 0.0413841 mole

Yield = 0.8781142

% yield = 87.811419

# APPENDIX E

# SIZE DISTRIBUTION OF SOLID PARTICLES

## $D_1$ Effect of Evaporation Temperature

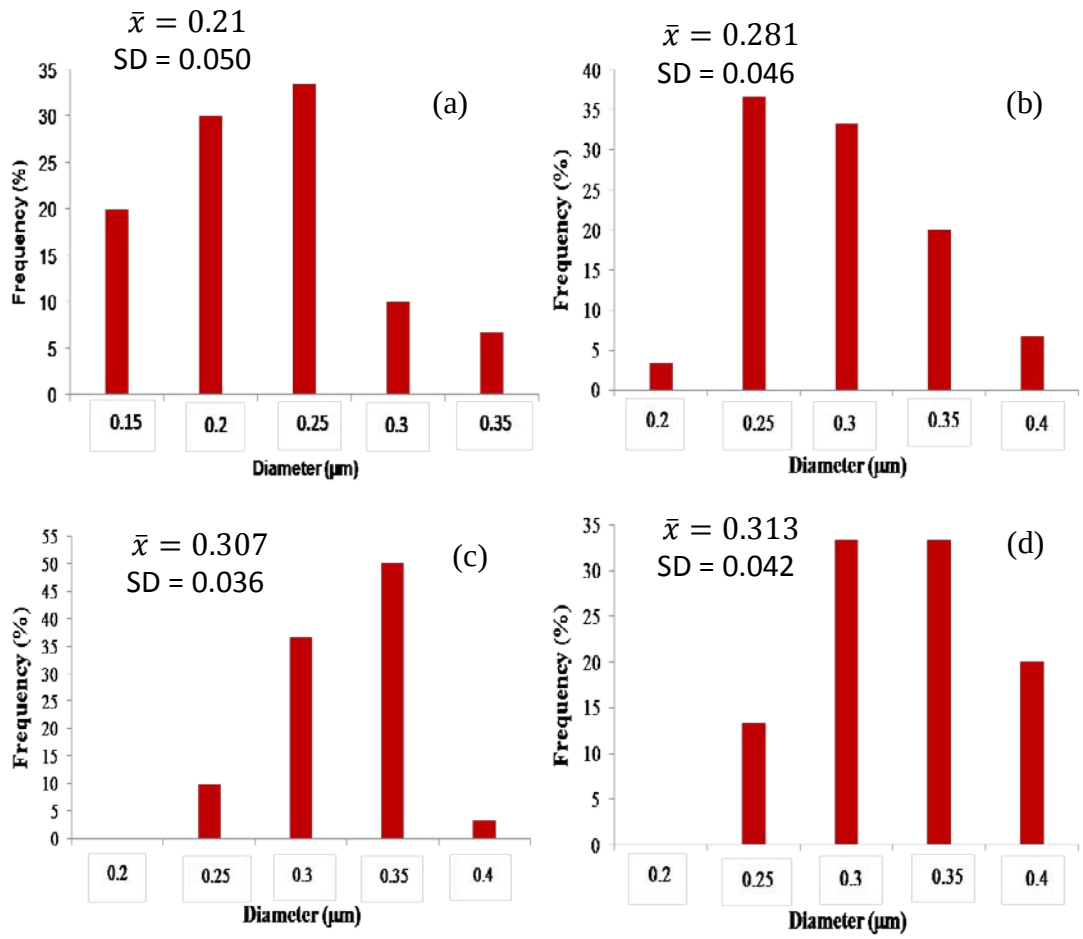


**Figure $D_1$** Frequency distributions for diameter of particles varying evaporation temperature; 650 $^{o}$C (a), 700 $^{o}$C (b), 800 $^{o}$C (c), 850 $^{o}$C (d)

**$D_2$ Effect of Zinc vapor Flow Rate**

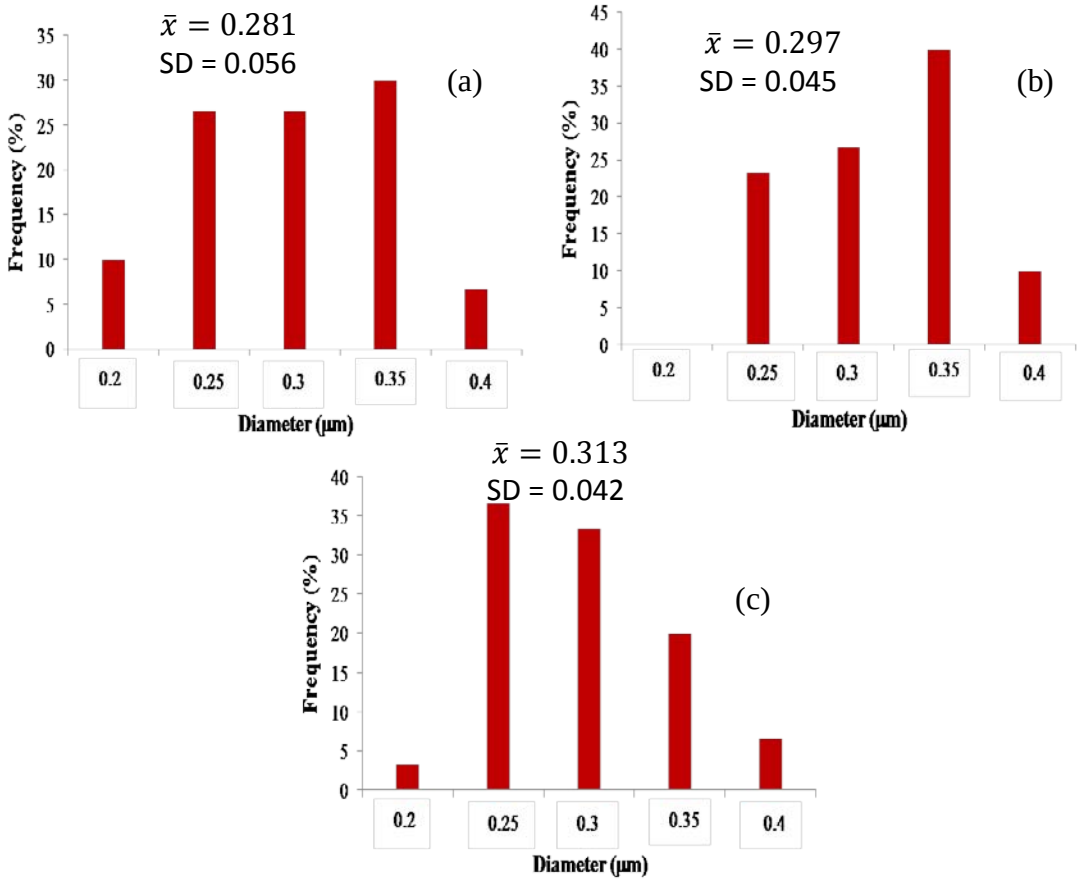


**Figure $D_2$** Frequency distributions for diameter of particles using zinc vapor flow rate; 0.5 l/min (a), 1 l/min (b) and 1.5 l/min (c)

**$D_3$ Effect of Reaction Temperature**

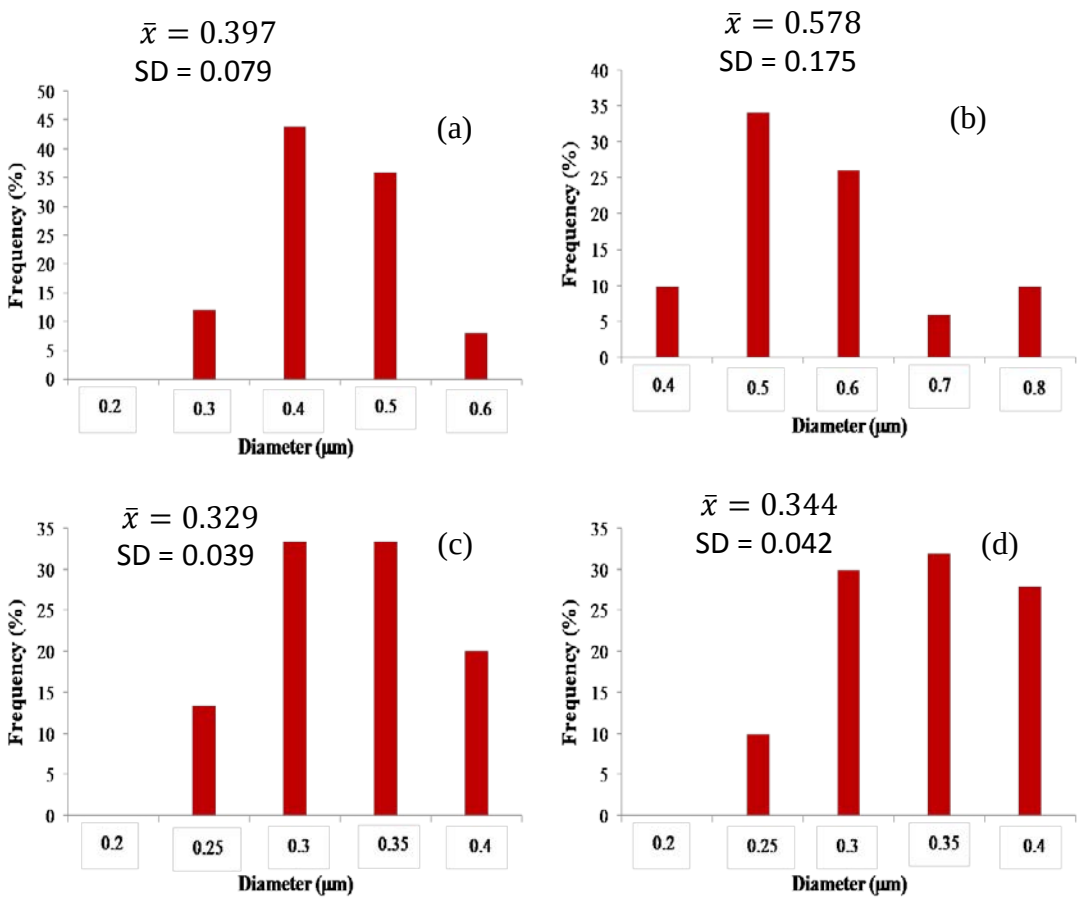


**Figure $D_3$** Frequency distributions for diameter of particles varying reaction temperature; 500 $^{o}$C (a), 600 $^{o}$C (b), 700 $^{o}$C (c), 800 $^{o}$C (d), 850 $^{o}$C (e) and 900 $^{o}$C (f).

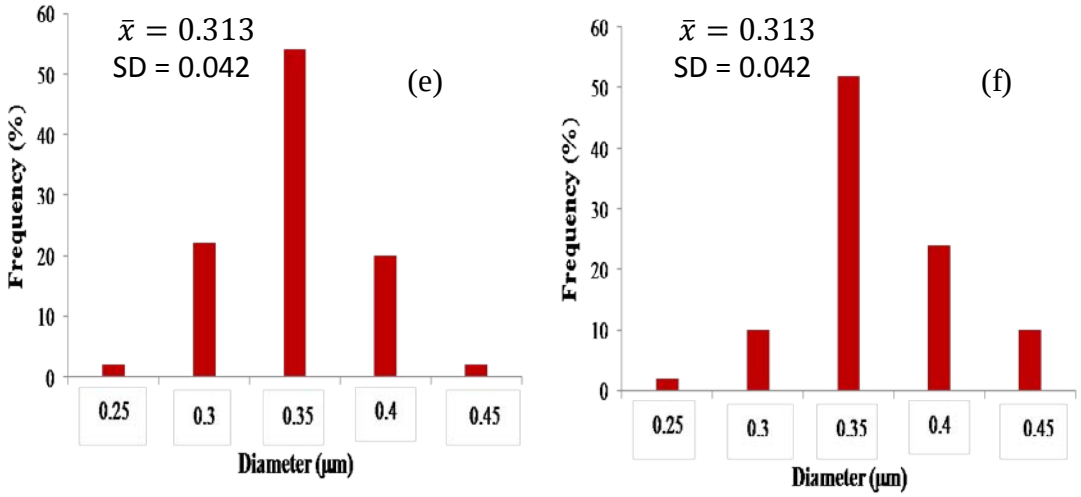


**Figure $D_3$** continue

# APPENDIX F

## Calculation of Zn balance

For example, in case of Ar carrier for steam flow rate 0.5 L/min and zinc vapor flow rate 0.5 L/min and $N_2$ gas flow rate 1 L/min. Zn raw material 3.361 g was exhausted in time 45 min under evaporation temperature 850 $^oC$ and reaction temperature 900 $^oC$.

| Equipment in the system | Wiegh of particles product (g) | Fraction of ZnO (wt) | Wiegh of ZnO product (g) | mole of ZnO product (mol) | Wiegh of unreacted Zn (g) |
|---|---|---|---|---|---|
| Reaction zone | 0.535 | 1.000 | 0.535 | 0.007 | 0.000 |
| Collecting tube | 0.601 | 0.910 | 0.547 | 0.007 | 0.054 |
| Chamber | 1.151 | 0.593 | 0.683 | 0.008 | 0.468 |
| Filter | 0.941 | 0.302 | 0.284 | 0.004 | 0.657 |
| Total | 3.228 | 2.805 | 2.048 | 0.025 | 1.180 |

$$Zn\ (g) + H_2O\ (g) \longrightarrow ZnO\ (s) + H_2\ (g)$$

From theoretical mole of ZnO was form equal mole of Zn was reacted

| | | | | | |
|---|---|---|---|---|---|
| Mole of Zn was reacted | = | 0.025 | mole | | |
| Weight of Zn was reacred | = | 1.643 | g | | |
| Weight of unreacted Zn | = | 1.180 | g | | |
| Total weigth of Zn | = | 2.823 | g | | |
| Weight of Zn foil | = | 3.361 | g | | |
| Weight of Zn loss | = | 0.538 | g | = | 16.019 % |

$$\text{Yield ZnO (yield actual/ yield theoretical)} = \frac{\text{mole of } ZnO_{ICP} * 100}{\text{mole of } ZnO_{max}}$$

$$\text{Yield ZnO (yield actual/ yield theoretical)} = \frac{0.025 * 100}{3.361/65.4}$$

$$\text{Yield ZnO (yield actual/ yield theoretical)} = 49.2 \ \%$$

# APPENDIX G

## Calculation of fully develop flow

Calculation flow rate of $N_2$ gas could be fully developed flow in the system. When inner diameter of pipe was 4.5 cm length of pipe was 34 cm and flow rate of $N_2$ gas was 1 l/min or 75.5 m/s.

$$E_l = \frac{L}{D}$$

L = length of pipe (cm)

D = diameter of pipe (cm)

$E_l$ = Entrance Length Number

$$E_l = \frac{34}{4.5}$$

$$E = 7.55$$

In the system was laminar flow

$$E_l = 0.06Re$$

$$Re = \frac{7.55}{0.06}$$

$$Re = 125.93$$

$$Re = \frac{\rho v D}{\mu}$$

$$\text{Velocity} = \frac{125.93 \text{x} 0.038}{1.735 \text{x} 4.5 \text{x} 10^{-2}} \quad \text{m/s}$$

$$\text{Velocity} = 64.21 \quad \text{m/s}$$

Then, velocity of 64.21 m/s was fully developed flow. However, in the system velocity was 75.5 m/s so flow rate of N2 gas could be fully developed flow.

# VITAE

Ms. Siriwimol Thanajirawat was born in Chonburi, Thailand, on February 7 1986. She studied in primary and secondary educations at Chonradsadornumrung School, Chonburi. In 2009, she graduated Bachelor Degree of Science (Chemical Technology) from Chulalongkorn University. After that, she continued to study in Master Degree in Center of Excellence in Particle Technology at Chemical Engineering Department, Faculty of Engineering, Chulalongkorn University with the research dissertation entitled “Simultaneous production of hydrogen and zinc oxide by hydrolysis of zinc vapor”